NAVAL POSTGRADUATE SCHOOL
Monterey, California
93940

D D C
RECEIVED
MAR 29 1972
B

| I FEB 1972   NPS-61Md 72021A |

Amplitude Modulation Of An
Acoustic Wave
Propagating Near The Sea Surface

Ocean Physics Group
W.J. Smith, Jr.   Physics Department

DOCUMENT CONTROL DATA - R & D

(Security classification of title, body of abstract and indexing annotation must be entered when the overall report is classified)

1. ORIGINATING ACTIVITY (Corporate author)	2a. REPORT SECURITY CLASSIFICATION
Naval Postgraduate School Monterey, California 93940	Unclassified
	2b. GROUP

3. REPORT TITLE

Amplitude Modulation of an Acoustic Wave Propagating Near the Ocean Surface

4. DESCRIPTIVE NOTES *(Type of report and inclusive dates)*

Technical Report, NPS-61Md72021A, February 1972

5. AUTHOR(S) *(First name, middle initial, last name)*

Wilton J. Smith, Jr.

6. REPORT DATE	7a. TOTAL NO. OF PAGES	7b. NO. OF REFS
February 1972	88	13

8a. CONTRACT OR GRANT NO.	9a. ORIGINATOR'S REPORT NUMBER(S)
b. PROJECT NO.	
c.	9b. OTHER REPORT NO(S) (Any other numbers that may be assigned this report)
d.	

10. DISTRIBUTION STATEMENT

Approved for public release; distribution unlimited.

11. SUPPLEMENTARY NOTES	12. SPONSORING MILITARY ACTIVITY
	Naval Postgraduate School Monterey, California 93940

13. ABSTRACT

Sixty kHz CW sound was propagated parallel to and near the ocean surface adjacent to an array of four thermistors, a salinometer, a sound velocimeter, a turbulent velocity probe, and a wave-height probe in order to investigate the statistics and environmental causes of amplitude modulation. The temporal variations of the sound amplitude were studied during four twenty-minute runs over a range of 2 meters at varying depths from near the surface to 14 meters during sea-state one conditions in water of 16 meters-depth. Analysis indicated mean percentage amplitude modulation of approximately 5% with a variance of approximately 10^{-3}. Temporal correlation times were about 2 seconds except for a 7 second time near the bottom. The power spectral densities of the modulation show strong components corresponding to predominant ocean wave frequencies as well as higher frequencies that may be attributed to bubble, temperature and/or salinity inhomogeneities. There is evidence that the microstructure dimensions are larger near the bottom than in the upper and middle depths.

14 KEY WORDS	LINK A		LINK B		LINK C	
	ROLE	WT	ROLE	WT	ROLE	WT
Acoustic Amplitude Modulation						
Ocean Acoustics						
Bubbles						
Near Surface Phenomena						
Oceanic Particle Velocity						

NAVAL POSTGRADUATE SCHOOL
Monterey, California
93940

I FEB 1972 NPS-6IMd 72021A

Amplitude Modulation Of An
Acoustic Wave
Propagating Near The Sea Surface

W.J.Smith, Jr.

Ocean Physics Group
Physics Department

NAVAL POSTGRADUATE SCHOOL
Monterey, California

Rear Admiral A.S. Goodfellow   M.U. Clauser
Superintendent   Provost
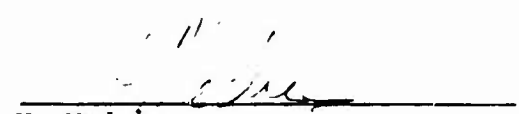
TITLE: Amplitude Modulation of an Acoustic Wave Propagating Near the
       Sea Surface - by W.J. Smith, Jr.

ABSTRACT:

Sixty kHz CW sound was propagated parallel to and near the ocean
surface adjacent to an array of four thermistors, a salinometer, a
sound velocimeter, a turbulent velocity probe, and a wave-height probe
in order to investigate the statistics and environmental causes of amp-
litude modulation. The temporal variations of the sound amplitude were
studied during four twenty-minute runs over a range of 2 meters at
varying depths from near the surface to 14 meters during sea-state one
conditions in water of 16 meters-depth. Analysis indicated mean per-
centage amplitude modulation of approximately 5% with a variance of
approximately 10^{-3}. Temporal correlation times were about 2 seconds
except for a 7 second time near the bottom. The power spectral densities
of the modulation show strong components corresponding to predominant
ocean wave frequencies as well as higher frequencies that may be at-
tributed to bubble, temperature and/or salinity inhomogeneities. There
is evidence that the microstructure dimensions are larger near the bottom
than in the upper and middle depths.

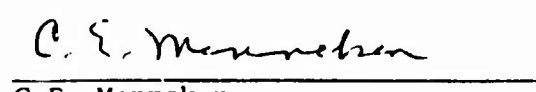Approved by:

H. Medwin
Professor of Physics
Coordinator of Ocean Physics Res.

Released by:

O. Heinz
Chairman
Department of Physics

C.E. Menneken
Dean of Research Administration

NPS-61Md72021A

1 February 1972

TABLE OF CONTENTS

ACKNOWLEDGMENT

I. INTRODUCTION

A. ACOUSTIC AMPLITUDE MODULATION IN A RANDOM MEDIUM

Consider an underwater acoustic wave propagated at a constant frequency and a fixed amplitude in isotropically homogeneous, undisturbed water with no scatterers. In the far field of the transducer, the wave will arrive at the receiver unchanged except for a diminution due to spherical spreading loss and absorbtion. The amplitude will not vary about the peak-to-peak value received. For low values of absorbtion, this type of acoustic wave is adequately described by the wave equation:

$$\nabla^2 P = \frac{1}{c^2}\frac{\partial^2 P}{\partial t^2}$$

Near the ocean surface, a wave will encounter random inhomogenieties which cause a varying speed of sound resulting in refraction. The wave equation must therefore be modified to include temporal and spatial changes in the speed of sound. Such changes may be expiessed as a change in the index of refraction $\mu(\vec{r},t)$, where $u(\vec{r},t)$ is the ratio of average sound speed to local sound speed:

$$\mu(\vec{r},t) = \frac{c_0}{c(\vec{r},t)}$$

which may be expressed as:

$$\mu(\vec{r},t) = 1 + \alpha\, n(\vec{r},t)$$

6

where α is the root-mean-square variation of the index of re-
fraction from unity, and $n(\vec{r},t)$ is the normalized variation of μ
from unity. The quantity α has been shown to be a small number,
equal to 1.18×10^{-4} in laboratory experiments using heated water
(Stone and Mintzer, 1965) and to 2.55×10^{-5} in ocean experiments.
(Whitmarsh, Skudrzyk and Urick, 1957.)

The effect of the random variation of the index of refraction
on an acoustic wave may be shown by a variation in the amplitude
of a received signal, noticable as a low frequency modulation of
the carrier frequency. Such modulation may be expressed as a
fraction of the maximum undisturbed amplitude of the received
signal as shown below:

$$\text{instantaneous fractional modulation} = \left[\frac{VMAX - VMOD}{VMAX} \right]$$

where

   VMAX = the unmodulated voltage value

   VMOD = the instantaneous modulated voltage value

The inhomogenieties which cause the variations in the re-
fractive index, and ultimately result in amplitude modulation, are
temporal and spatial variations in temperature and salinity micro-
structure, random bubble populations, particulate matter, varying
forms of oceanic life and those inhomogenieties caused by man.
Each factor will vary with location and ambient conditions in the
ocean. The effect on sound transmission may also be a function of
sound frequency.

Particle velocit in the ocean has a great effect on the above
parameters, generally in determining their temporal and spatial

7

distribution. There are two main types of oceanic particle velocity, that due to convective turbulence and that due to the effect of surface waves. Convective turbulence is fairly slow and affects the distribution of temperature and salinity. Such concepts as temperature "patches" and lenticular volumes of near unitemperature are due to convective turbulence.

Turbulence arising from the effect of surface wave action is generally responsible for random variations in populations of scatterers and for small scale variations in temperature and salinity distribution.

Distribtuions and variations of all parameters affected by wave turbulence would show a lessening effect with increasing depth due to the e^{-kz} decay of wave amplitude. Convective turbulence could exist at all depths near the surface and its dependence on depth is unknown. These mechanisms are always present near the surface of the ocean and are a principal factor in the modulation of sound. They also lead to problems in analysis. For example, a stationary temperature patch might show temporal characteristics due to displacement across a sensor with wave action.

Statistical analysis of the amplitude modulation occurring in inhomogeneous transmission has centered about the coefficient of variation, CV, defined by Stone and Mintzer (1961):

$$(CV)^2 = \frac{(\langle P^2 \rangle - \langle P \rangle^2)}{\langle P \rangle^2}$$

where   CV = the coefficient of variation

      P = the amplitude of the received signal

      $\langle \ \rangle$ = the ensemble average.

8

The same coefficient of variation is defined equivalently by Campanella and Favret (1969) as:

$$(CV)^2 = \left[\frac{\langle S(t) - \langle S(t) \rangle \rangle}{\langle S(t) \rangle} \right]^2$$

where S(t) is the amplitude of the received signal.

The relationship between the coefficient of variation as defined by Stone and Mintzer, (CV), and the fractional modulation as defined in this thesis is shown in Appendix I.

The relation between $(CV)^2$ and the RMS variation of the index of refraction α, the range r and the size of the inhomogenieties has been variously described, as by Stone and Mintzer (1965) depending on the (presumed) shape of the spatial correlation function of the index of refraction $R(\rho)$ where:

$$R(\rho) = \langle n(\vec{r}) n(\vec{r} + \rho) \rangle$$

If $R(\rho)$ is Gaussian,

$$R(\rho) = \exp(-\rho^2 / a^2)$$

then the coefficient of variation may be derived for the conditions that

$$kr \gg 1$$
$$ka \gg 1$$

and, $r/ka^2 \ll 1$

as:

$$(CV)^2 = \frac{1}{2} \sqrt{\pi} \, k_0^2 \alpha^2 a r$$

where k_0 = space wave number of the sound frequency

α = RMS variation of the index of refraction

a = radius of the scattering inhomogeniety

r = transducer to receiver range.

9

If $R(\rho)$ is exponential;

$$R(\rho) = exp(-\rho/a)$$

then the numerical factor in the expression for $(CV)^2$ above would be unity. Although an exponential correlation function would not satisfy the requirements of non-zero slope at $\rho = 0$, the experimental work (Stone and Mintzer, 1961 and 1965, and Campanella and Favret, 1969) seems to indicate an exponential correlation function. The dilemna can be resolved by using a modified exponential function to satisfy the $\rho = 0$ condition.

The temporal correlation function for the variation of the index of refraction,

$$M(\tau) = \langle n(t) n(t+\tau) \rangle$$

has been compared to the temporal correlation function for the variation of sound pressure amplitudes,

$$\phi(\tau) = \langle S(t) S(t+\tau) \rangle$$

and the relation:

$$M(\tau) = \phi(\tau)$$

which was derived theoretically by Mintzer (1954) and was shown to exist experimentally by Campanella and Favret (1969) in a controlled laboratory environment using convective temperature differences to generate a varying index of refraction.

Experimental work in the ocean environment has included propagation at frequencies from 800 Hz (R.M. Kennedy, 1969) and 60 kHz (Whitmarsh et al., 1957) at distances of 1000 yds (Whitmarsh et al.) and twenty-five miles. (Kennedy.)

10

Kennedy found the probability distribution function of the
logarithm of the amplitude fluctuations to be normally distributed,
and an exponential temporal correlation function with an average
decorrelation time to 1/e in 12 minutes. There was no attempt to
take measurements of the environment during his experiment.
Whitmarsh, Skudrzyk and Urick found that the fluctuation in amp-
litude tended to increase with range, and decried a lack of good
information concerning the microthermal structure of the ocean.

B. SCOPE AND INTENT OF THE EXPERIMENT

The purpose of the experiment was to measure and analyze the
temporal variation in the fractional modulation of an acoustic wave
over an oceanographically defined volume in the ocean. The tem-
poral characteristics of the environmental factors of temperature,
salinity, turbulent velocity, sound speed and wave height were
measured simultaneously with fluctuations in sound amplitude.

A simple one-transducer and hydrophone arrangement over a
short transmission length of two meters was adequate to measure
variations in the amplitude of the transmitted signal. The short
range was desirable because of the need for system rigidity and an
adequate definition of the environmental factors occurring during
each twenty-minute run. The length of each run was the minimum
time necessary to statistically define the low frequency environ-
mental factors which caused the amplitude modulation.

The acoustical and oceanographic analysis at each depth was
concerned with the statistical and temporal characteristics. The
results desired were the mean and variance, the probability density
function, the temporal correlation and the power spectral density
of each variable.

11

The acoustic results will later be cross-correlated with the varying environmental factors to determine the relative effect of each parameter upon the amplitude modulation.

II. DESIGN OF THE EXPERIMENT

A. DETERMINATION OF THE CONFIGURATION OF THE EXPERIMENTAL APPARATUS

1. Conceptual Design of the Experiment

In order to measure environmentally caused amplitude modulation over a clearly defined volume in the ocean, a high frequency acoustic carrier wave was directed at a receiving hydrophone mounted upon the acoustic axis at a separation of two meters. The received signal was processed for the amplitude modulation occurring in each twenty-minute run.

In support of the acoustic investigation, an electromagnetic flowmeter, three thermistors, a Bissett-Berman apparatus with a salinometer and a temperature probe and a Ramsey probe with a velocimeter and a wave-height probe were mounted about the acoustic apparatus to define the environment during each run.

2. The Acoustic Carrier Wave

The carrier wave utilized in the experiment was a continuous-wave 60 kHz constant amplitude signal. This frequency selected in order to maximize the effect of random bubble populations which were anticipated to be greatest near the ocean surface.

As may be seen from Figure II-1, the 60 kHz carrier frequency was near resonance for the most populous bubble sizes near the surface. The resonance curves were calculated on the basis of the formula:

$$f_0 = \frac{1}{2\pi R_0} \sqrt{\frac{3\gamma P_0}{\rho_0} \frac{\gamma}{\alpha}}$$

13
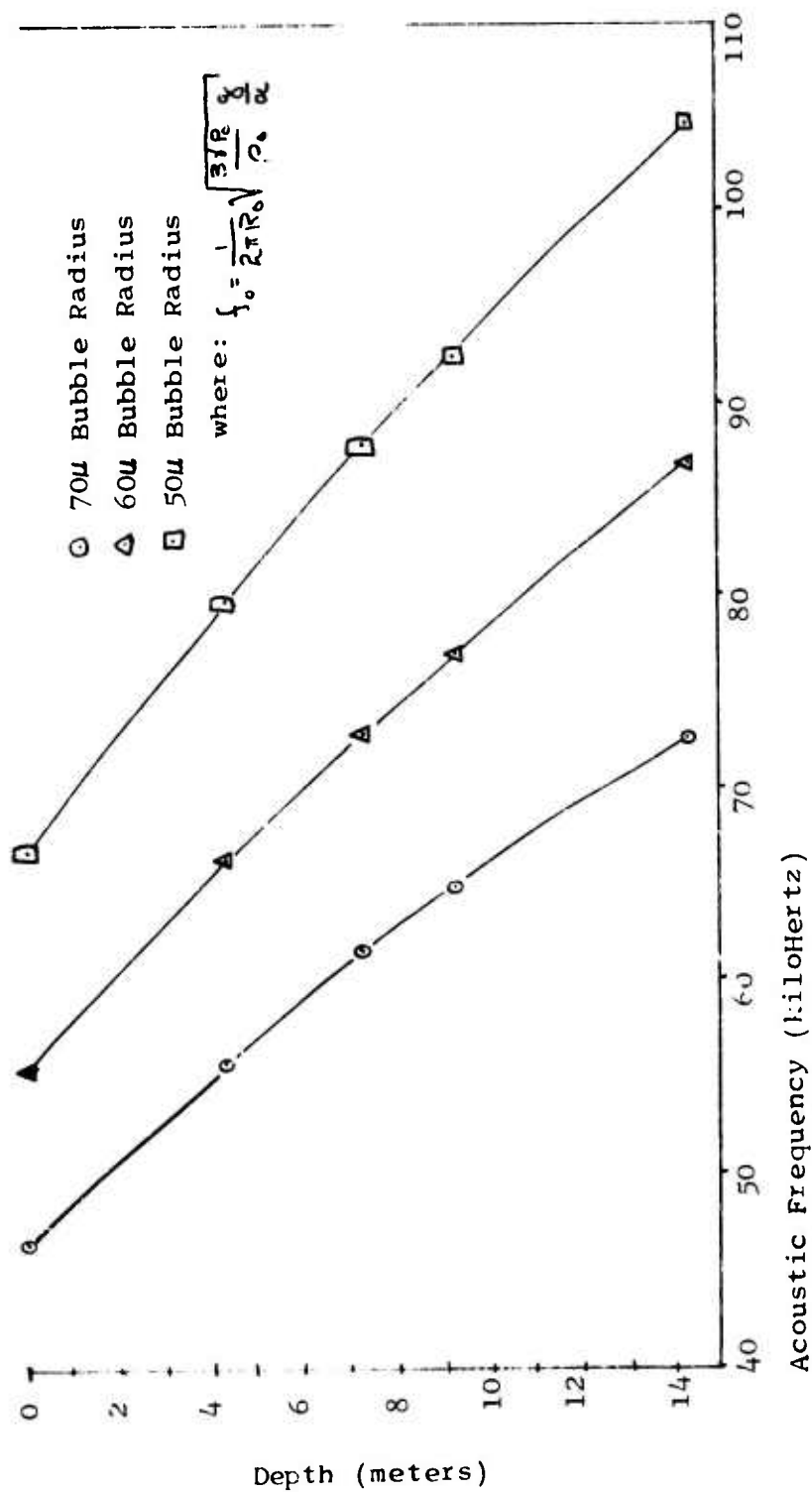
BUBBLE RESONANT FREQUENCY VERSUS DEPTH

Figure II-1

14

where f_O = resonance frequency (Hz)

R_O = radius of the bubble (cm)

F_O = ambient pressure at the bubble depth, equals 10^6 dynes/cm^2 at the surface with 10^6 dynes/cm^2 added for each 10 meters of depth

ρ_O = density of water (1.0 gram/cm^3)

γ = ratio of specific heats (assumed to be 1.4)

$_G\alpha^{-1}$ = correction for surface tension and thermal conductivity equals 1.0296 for 60 kHz

3.   Determination of the Acoustic Range

The most stringent requirements for the distance between transducer and hydrophone arose from the desirability that

(a) the hydrophone be in the far field of the transducer.

(b) the volume of water under investigation be locally defined in terms of the measurable parameters of temperature, salinity, speed of sound and surface wave height.

(c) the mounting of the hydrophone be stiff enough to preclude significant changes of sound amplitude through the sound beam.

(d) the path length be long enough to observe measurable amplitude modulation.

The compromise transducer to hydrophone distance was set at two meters. Checking requirement (a), for the available source (F-27) using the criterion $r = a^2/\lambda$, and assuming an average sound speed of 1500 meters a second;

$$f = 60 \times 10^4 \text{ Hz}$$
$$\lambda = c/f = (1500/6) \times 10^{-4} = 2.50 \times 10^{-2} \text{ meters}$$
$$a = 0.127 \text{ meters, where a is the radius of the transducer face}$$

15

then, the far field begins at (approximately)

$$r = a^2/\lambda = 0.01613/0.0250 = 0.645 \text{ meters}$$

Thus the far field begins well within the two meter distance between the transducer and the hydrophone.

For requirements (b) and (d) the two meter distance was selected to be long enough to yield measurable amplitude modulation, yet short enough to allow oceanographic measurements on a definable volume of water. The data from the runs proved this selection to be justified.

The alignment of the receiving hydrophone with the acoustic axis of propagation was an important consideration. A narrowly defined beam pattern reduced reflection from the apparatus, but a radius of error had to be calculated in order to establish the effect of minute movement of the receiver (requirement (c)).

Pressure amplitude as a function of angle was calculated from the formula below, where only the last term is important;

$$P = j\rho_o c \left[\frac{ka^2}{2r}\right] u_o e^{j(\omega t - kr)} \left[\frac{2 J_1 (ka\sin\theta)}{ka\sin\theta}\right]$$

For one per cent modulation, an angular displacement of 0.45^o would have to occur, two meters, the radius of movement would be;

$$\theta = 0.45^o$$

$$\sin\theta = x/2 \text{ meters}$$

$$x = 2(0.0075)$$

$$x = 0.0150 \text{ meters}$$

The radius of movement would have to be 1.50 centimeters, more movement than the mounting would allow. As a final test at

the scene of the experiment, a diver "twanged" the hydrophone
supporting wire with no observable result in amplitude modulation.
It is estimated that no more than 0.1% modulation could be caused
by movement of the hydrophone by ocean forces.

4. Design of the Apparatus

The apparatus (see Figure II-2) as designed was a square
of height six feet and length two meters from the face of the
transducer to the receiving hydrophone.

Three sides of the mount were of two inch diameter steel
pipe and the fourth was one-eighth inch steel wire stretched by
means of steel springs to a tension of one hundred and fifty
pounds.

The square shape offered two distinct advantages, the
shortness of the horizontal members minimized vibratory "tuning
fork" effects in conjunction with the tension in the wire; it
also minimized the number of reflection paths from source to
receiver Acoustic absorbent rubber (SoAB) mounted for eighteen
inches along the upper and lower members also reduced possible
reflections to the point that reflections were down 38 db relative
to the signal when a pulsed 60 kHz signal was propagated.

An eleven inch steel disc was welded to the vertical pipe
member directed perpendicularly to the sound axis as a mount for
the transducer.

The completed design combined two necessary characteristics,
rigidity and minimum self-generated hydrodynamic turbulence. The
end of the apparatus holding the transducer was necessarily
massive to insure rigidity about the propagating transducer.

17
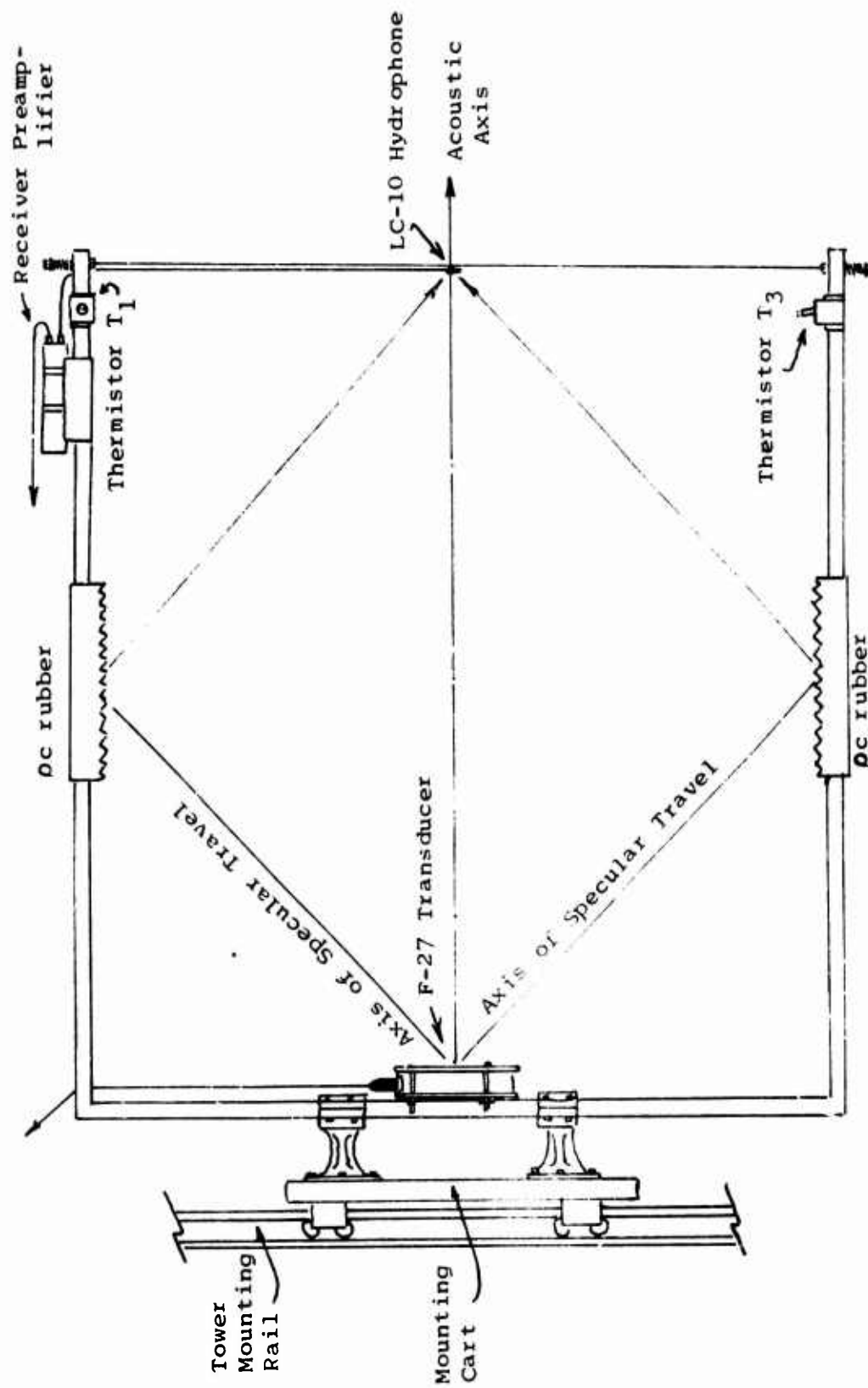
ACOUSTIC APPARATUS IN EXPERIMENTAL CONFIGURATION

Figure II-2

18

Hydrodynamic turbulence scattered from the transducer was kept to a minimum by having the sound source end of the entire apparatus face the mean current.

The wire served as the mounting for the receiving hydrophone. Since the hydrophone was quite light in weight, the wire was rigid enough, while the small size of the wire precluded any significant hydrodynamic turbulence.

5. The Transducer

The transducer utilized was the USRD type F-27. The transmitting array consists of fifty-five one-inch diameter lead metaniobate discs 0.22 inches thick, each of which is cemented to a one-inch diameter, $\frac{1}{2}$ inch thick tungsten backing plate which acts approximately as a circular piston.

The F-27 transducer was designed for wide range unidirectional underwater sound projection at a frequency range of one kilohertz to forty kilohertz. The USRD recommends a limit of forty kilohertz since the beam pattern was considered to be too sharp at higher frequencies. This characteristic was advantageous to the experiment at sixty kilohertz and results were indicative of proper transducer selection, with the one-half power points measured at three degrees off the sound axis, and the side lobes at sixty degrees down forty db from the axial sound pressure level.

6. The Receiving Hydrophone

The experiment required a small, sensitive hydrophone. The hydrophone used was the Atlantic Research Corp. type LC-10 with a diameter of 0.635 centimeters. For the sixty kilohertz carrier wave, the wavelength is 2.50 cm, making the wavelength 3.95 times

the diameter of the hydrophone. The sensitivity of the LC-10 is -110 dB re 1 volt per microbar at 60 kHz. The hydrophone was mounted vertically along the wire, with the central part of the cylinder perpendicular to the sound axis.

B. PROCESSING ELECTRONICS

1. Overall System Operation

The processing electronics were designed to present the waveform of the amplitude modulation taking place on the acoustic carrier wave over a dynamic voltage range compatible with that of the recording equipment. Generally, it was desired to present a ten volt peak-to-peak signal at the entry leads of the envelope detector, and then process the waveform to view only the amplitude modulation. (See Figure II-3.)

The 60 kHz wave was originated in a GR 1162A frequency synthesizer which produced a one volt to four volt peak-to-peak waveform accurate and constant to within one millivolt over extended periods of operation.

The carrier waveform was then amplified to the voltage necessary to produce a ten volt peak-to-peak waveform at the envelope detector by an HP 467A power amplifier set at a fixed "times ten" setting. It was found to be advantageous to set the power amplifier at a fixed output and vary the output of the GR 1162A frequency synthesizer in order to achieve the desired voltage value at the envelope detector.

The power-amplified signal was then transmitted through one hundred and fifty feet of waterproof cable to the F-27 transducer and transmitted to the LC-10 receiving hydrophone.

20
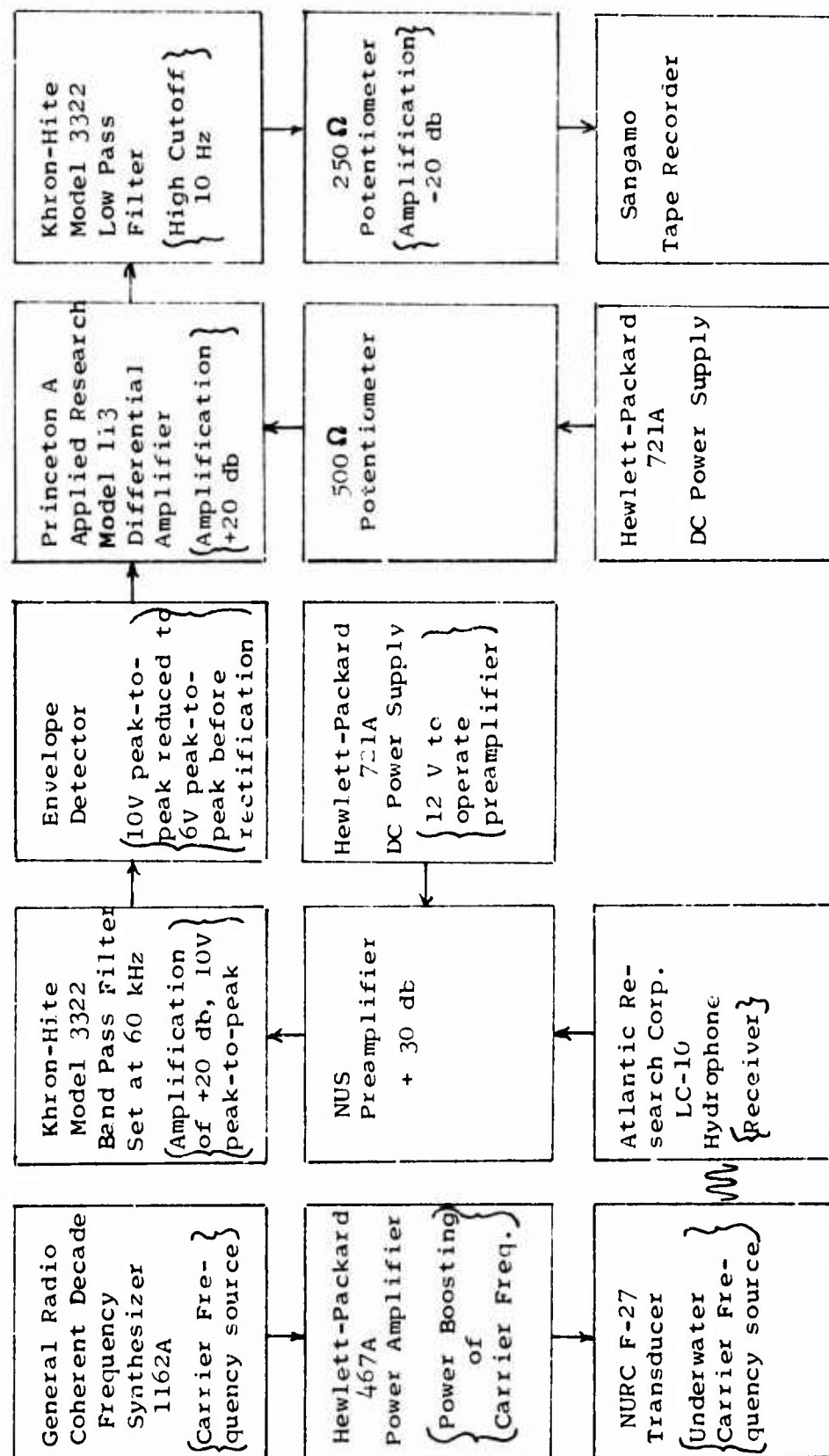
ELECTRONICS PROCESSING AND DATA GATHERING SYSTEM CONFIGURATION

Figure II-3

21

The signal as received by the LC-10 hydrophone was amp-
lified by a fixed +30 db (x 31.6) gain NUS model 2010-030 voltage
preamplifier in a watertight can mounted on the upper horizontal
member of the mounting apparatus. The preamplifier required a
twelve volt DC input, supplied by a Hewlett-Packard 721A DC power
supply. The amplified signal was transmitted through one hundred
and fifty feet of watertight cable to the initial electronic pro-
cessing equipment.

The initial processing of the modulated waveform consisted
of bandpass filtering the signal with a center frequency of 60 kHz
through a pass band of $\pm$ three hundred Hertz, with -24 db per
octave attenuation on either side of the pass band. The unit
utilized was the Khron-Hite model 3322 variable filter. In order
to arrive at a ten volt peak-to-peak waveform at the output of
the filter, a +20 db internal amplification feature of the filter
was utilized. The output at this point consisted of a ten volt
maximum peak-to-peak voltage with a low frequency environmental
amplitude modulation superimposed upon it, varying to a maximum of
sixteen per cent of the peak wave form.

The above waveform was processed to detect the modulation
by the envelope detector (see Figure II-4) described in detail in
the following section. The salient point is that the ten volt
signal was reduced by a factor of 0.6 in the audio transformer of
the envelope detector.

The output of the envelope detector was the varying voltage
induced by the amplitude modulation superimposed upon a small
amount of DC voltage.

22
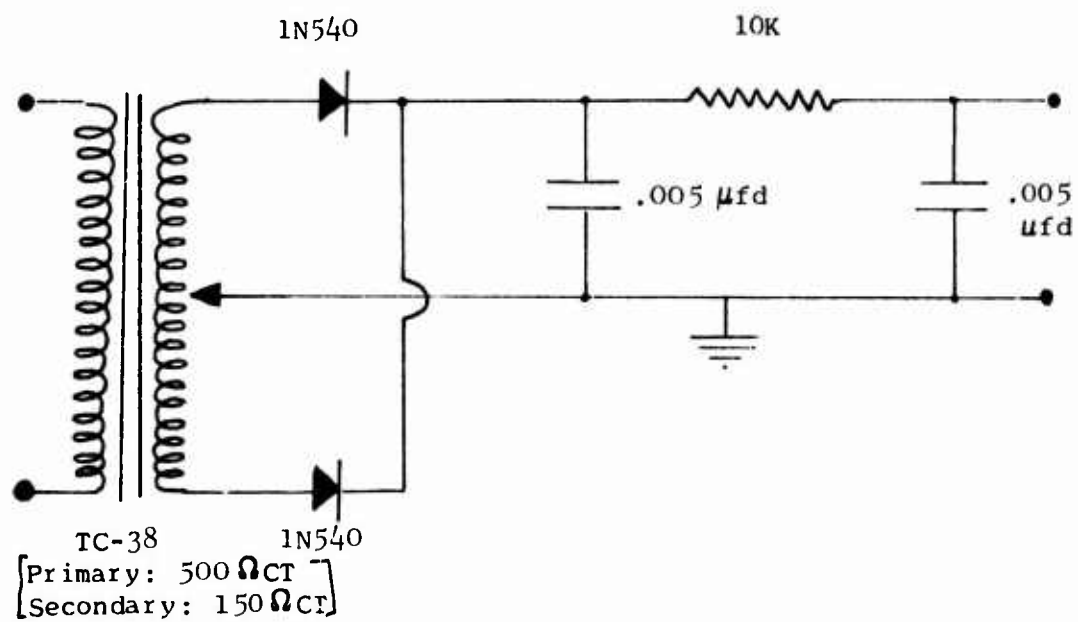
CIRCUIT DIAGRAM OF THE ENVELOPE DETECTOR

Figure II-4
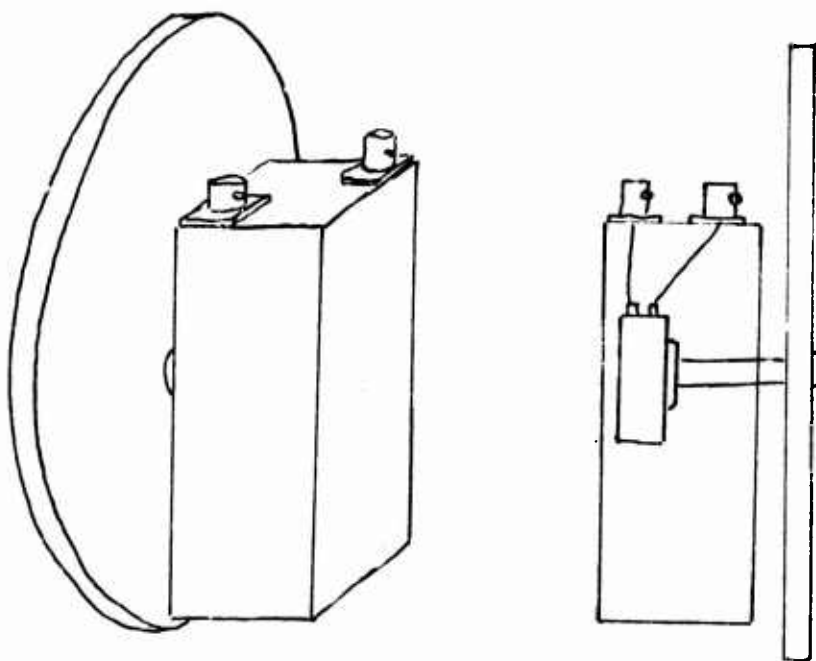
DC COMPENSATION VOLTAGE POTENTIOMETER

Figure II-5

The envelope detector output was led into the positive input jack of a PAR Type 113 differential amplifier. The differential amplifier was used to eliminate the DC component of the amplitude modulation waveform. This was accomplished by simultaneously placing a DC voltage into the negative input jack. The DC voltage was supplied by an HP 721A DC power supply set at an output of four volts and reduced by means of a 500 ohm potentiometer to that (negative) voltage required to reduce the amplitude modulation to a purely alternating signal.

The potentiometer was necessary to assure a constant DC input level. The power supply/potentiometer combination was tested over a continuous two hour period with less than a one millivolt variation during the entire period. The potentiometer was configured with an outsized tuning wheel to allow minute (less than one millivolt) adjustments of the DC compensating voltage. (See Figure II-5.)

The compensated amplitude modulated signal was amplified by a factor of ten in the differential amplifier which made the varying voltage too high for the tape recorder, but which was subsequently reduced by a potentiometer. The ten-times setting was the minimum amplitude setting on the PAR 113.

The signal was subsequently passed through another Khron-Hite 3322 filter set in a four-pole Butterworth low pass configuration with a high cutoff of ten Hertz and a minimum frequency of 0.001 Hertz. The attenuation at the high frequency end was -48 db per octave. The internal amplification feature was not utilized.

24

The lowpass-filtered amplitude modulation signal was re-
duced to allow dynamic voltage range compatibility with the tape
recorder. The reduction was accomplished by the use of a 250 ohm
potentiometer set to reduce the low-pass filter output by a factor
of ten. This reduction had the desirable result of restoring the
amplitude modulation to its value relative to the six volt output
of the audio transformer in the envelope detector.

The signal was recorded on a Sangamo model 3500 fourteen
track tape recorder simultaneously with the oceanographic mea-
surements during each run. The dynamic range of the tape recorder
in the FM mode utilized was 0.01 to 2.50 volts, with all the amp-
litude modulation observed falling within this range.

The electronic processing design proved to be quite
satisfactory except for details in various components which were
amply compensated for during the course of the experiment.

2. The Envelope Detector

The envelope detector was adapted from an ocean wave height
detector and proved to be satisfactory. The detector is essentially
a double rectification device with an RC filter and a capactive lead
to ground potential to discharge DC voltages built up in the sili-
con diode (1N540) rectifying elements. (See Figure II-4.)

The time constant for the RC filter at a carrier fre-
quency of 60 kHz is fifty microseconds and with double rectifi-
cation there was no appreciable decay between peaks.

The envelope detector proved sensitive to acoustic modu-
lation of as little as one twentieth of one per cent in the
laboratory tanks.

25

Possible improvements to the detector would be the sub-
stitution of larger capacitors in the filtering element to reduce
the substantial (1.3 volt) DC component in the output.

III. EXPERIMENTAL PROCEDURE

A. GENERAL

The amplitude modulation runs were performed on the twenty-first of October 1971 at the NUC Oceanographic Research Tower at San Diego. The runs were twenty minutes in length, to allow enough time for major low frequency ocean phenomena to be adequately described and measured.

The ocean sensors were mounted around the acoustic sensors in o··'er to define the volume of ocean over which the amplitude modulation took place. (See Figure III-1.) The sensors were selected to measure temporal variations of temperature, salinity, turbulent velocity, wave height and the speed of sound during the period of acoustic measurement. During each run, the oceanographers present also measured and observed weather and sea surface conditions as background for the more precise information presented by the ocean sensors. The ocean sensors used are listed below with respect to the parameters they measured.

1. Temperature

a. Three thermistors located about the apparatus obtained temporal variation of temperature in the volume of water under observation.

b. One Bisset-Berman temperature sensor measured absolute values of temperature near the F-27 transducer over a range of $14^{\circ}C$ to $19^{\circ}C$.

27
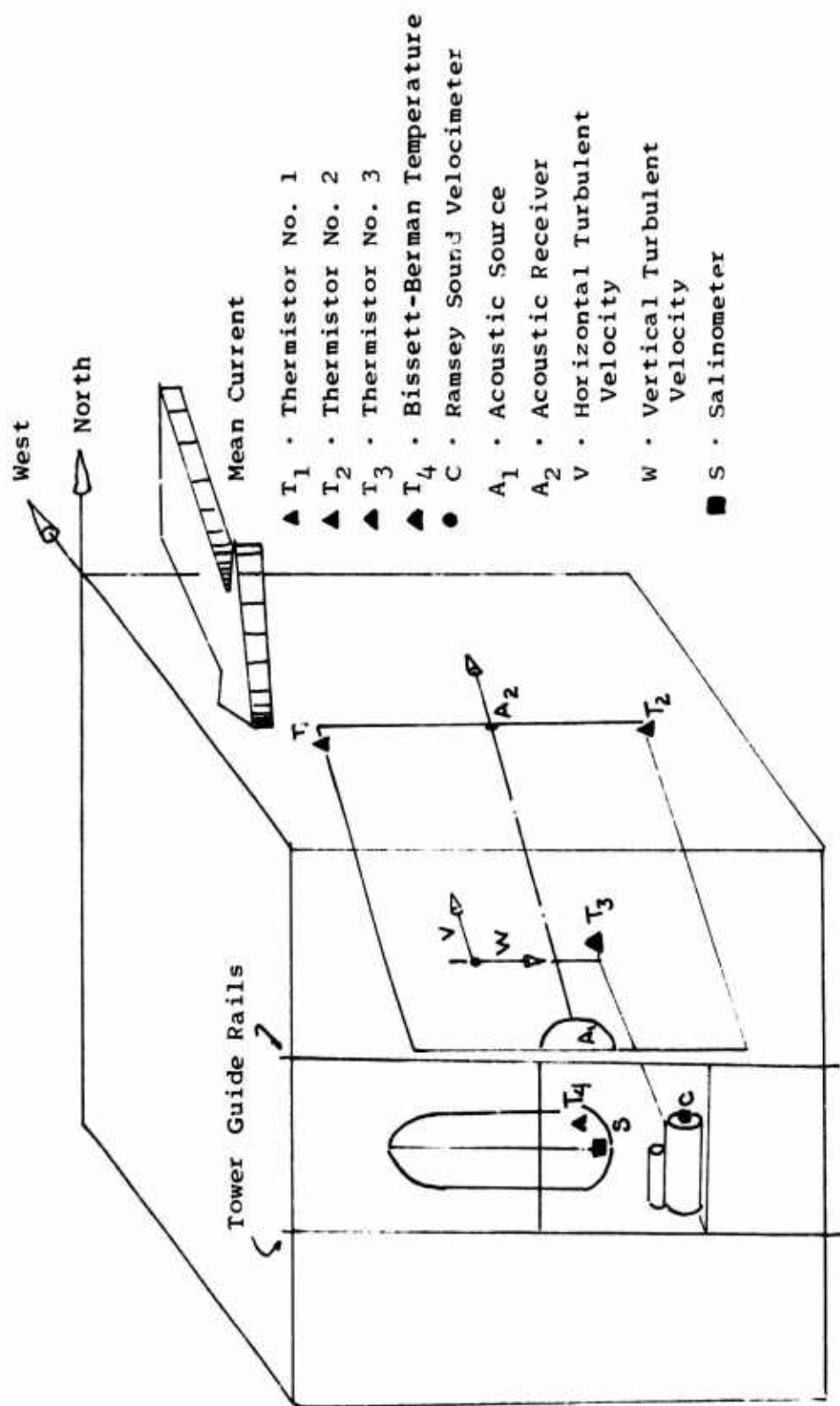
SPATIAL CONFIGURATION OF ACOUSTIC AND OCEAN SENSORS IN RELATION TO WATER VOLUME, MEAN CURRENT AND CARDINAL BEARINGS (LESS SOME DETAIL)

Figure III-1

West

North

Mean Current

▲ T_1 · Thermistor No. 1
▲ T_2 · Thermistor No. 2
▲ T_3 · Thermistor No. 3
▲ T_4 · Bissett-Berman Temperature
● C · Ramsey Sound Velocimeter

A_1 · Acoustic Source
A_2 · Acoustic Receiver
V · Horizontal Turbulent Velocity
W · Vertical Turbulent Velocity
■ S · Salinometer

Tower Guide Rails

28

2. Salinity

One Bisset-Berman salinometer located near the F-27
transducer measured temporal variation in salinity over a range
of 37.5 to 39.5 parts per thousand.

3. Particle Velocity

An electromagnetic flowmeter measured one component, (u)
or (v), of horizontal velocity and the vertical component (w). The
flowmeter was located about one-half of the distance between the
acoustic sensors 1.13 meters downstream from the acoustic axis.

4. Speed of Sound

The sound speed was measured as an absolute value with
temporal variations by a Ramsey Corp. Mark I SVTD probe located
near the base of the acoustic apparatus.

5. Wave Height

The wave height was measured by two sensors, a pressure
wave height indicator and a Baylor gauge.

As noted above, not all the ocean sensors were operating
during all runs. Five runs were made, with runs two through four
considered suitable for analysis. The general scheme was to per-
form two runs near the surface, the first run with the electro-
magnetic flowmeter measuring in the u and v (horizontal)
directions, and the second with the flowmeter measuring in the u
and w (or vertical) directions. Three runs followed at deeper
depths with the flowmeter in the u-w configuration. The first
run was aborted when the flowmeter malfunctioned, but runs two
through five proved to be successful. A listing of the runs taken
is presented below; all times are local and the date is 21 October

29

1971. Mean water level was 6.7 meters below the concrete deck of the NUC tower. The depths are in meters below mean water.

Run 1.

depth: 4.3 meters,

times: start: 1419 stop: 1439

comment: The data from this run were not analyzed due to a malfunction of the electromagnetic flowmeter.

Run 2.

depth: 4.3 meters,

times: start: 1530 stop: 1550

sensors: turbulence: 1. u (horizontal) velocity

2. w (vertical) velocity

3. sound velocity

4. Both wave heights

temperature: 1. thermistor T_3

2. Bissett-Berman temperature

salinity: 1. Bissett-Berman salinometer

Run 3.

depth: 9.3 meters,

times: start: 1616 stop: 1636

sensors: turbulence: 1. u velocity

2. w velocity

3. sound velocity

4. both wave heights

temperatures: 1. thermistors T_1, T_2, and T_3

2. Bissett-Berman temperature

salinity: Bissett-Berman salinometer

Run 4.

   depth: 14.3 meters,

   times: start: 1648 stop: 1708

   sensors: all sensors operating, see sensor information

for Run 3.

   Run 5.

   depth: 7.3 meters,

   times: start: 1728 stop: 1748

   sensors: all sensors operating, see sensor information

for Run 3.

B. CONFIGURATION OF THE OCEAN SENSORS IN RELATION TO THE ACOUSTIC
    APPARATUS

Two factors determined the configuration of the ocean sensors

relative to the acoustic apparatus. First, the volume of water

around the acoustic axis had to be described adequately for

temporal variations, and second, the ocean sensors had to be

placed such that there was little or no interference from down-

stream turbulence from the sensors themselves.

Temperature variations and turbulent velocities were considered

to be the most important parameters affecting the amplitude modu-

lation. Temperature variations were recorded by the three ther-

mistors and the Bissett-Berman temperature probe. The Bissett-

Berman probe was placed centrally between the acoustic apparatus

and the mount for the flowmeter due to its size. Two of the ther-

mistors were placed above and below the receiving hydrophone in the

vertical plane of the acoustic axis, while the third was placed

along the horizontal plane of the axis midway between the trans-

ducer and the hydrophone. (See Figure III-2.)

31

Mean Current

Bissett-Berman Probe

Electromagnetic
Flowmeter

Ramsey Probe

Thermistor 1

LC-10 Hydrophone

Thermistor 2

Thermistor 3
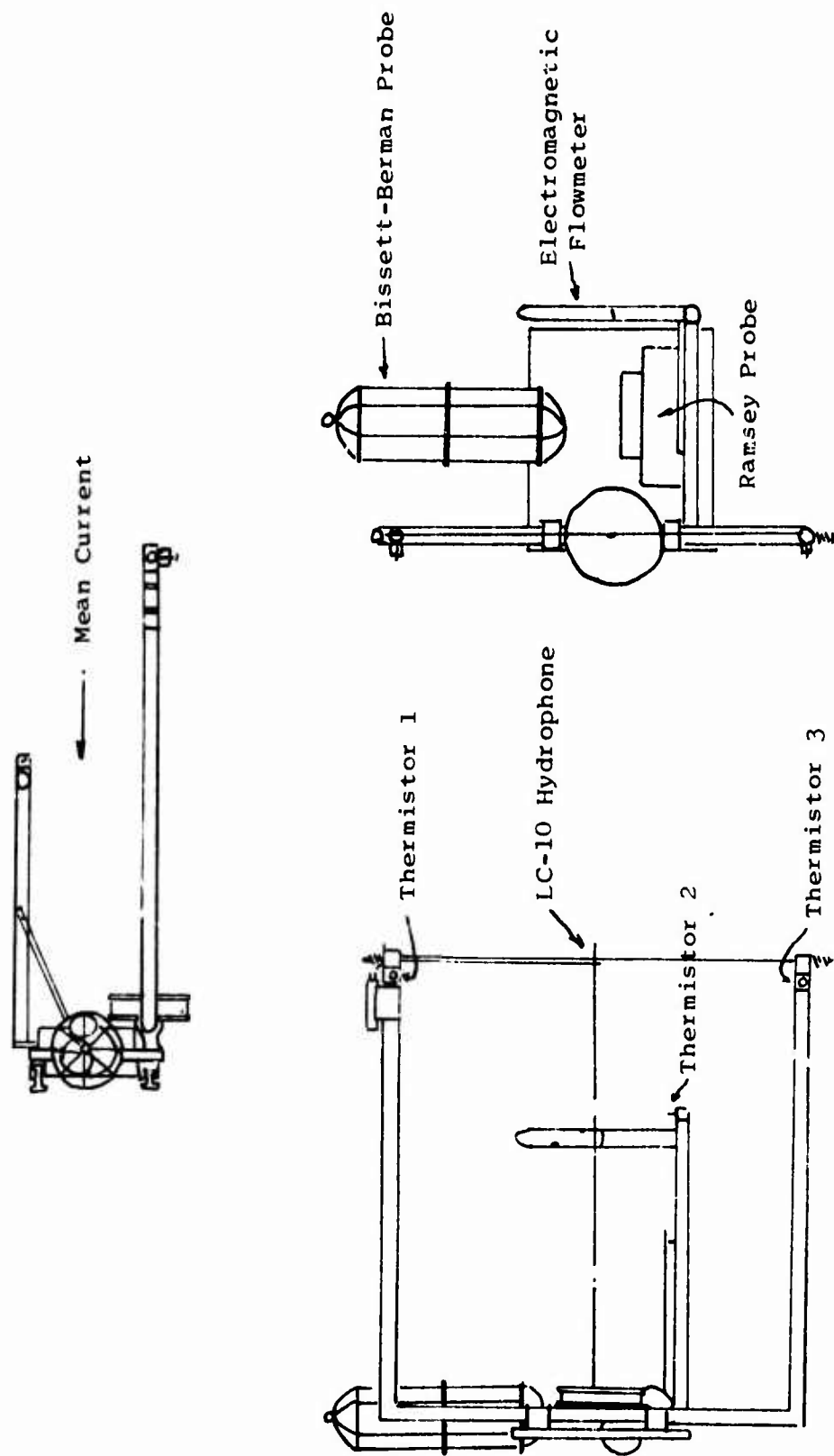
CONFIGURATION OF ACOUSTIC AND OCEAN SENSORS DURING THE
EXPERIMENTAL RUNS

Figure III-2

32

The electromagnetic flowmeter was placed so that it measured the turbulence occurring 113 centimeters from the center of the acoustic axis.

All other sensors were integral parts of large instruments and were placed between the acoustic apparatus and the mount for the flowmeter to minimize the effect of their wake turbulence.

Figure III-3 shows the distances between various sensors. The mean current was as shown in Figure III-1, with the apparatus up-stream of all other equipment.

C. DETERMINATION OF RUN DEPTHS

The mean water depth at the NUC tower was 16.4 meters (54 feet) during the time of the runs. Four depths were selected in order to observe near-surface to near-bottom amplitude modulation effects. The first two runs were at an estimated water depth of 4.3 meters, the third at an estimated 9.3 meters, the fourth (and deepest) at 14.3 meters, and the last run was at 7.3 meters.

These depths were chosen in order to cover the entire water column and to minimize interference from the underwater beam structure of the tower. The shallowest depth was far enough from the surface to avoid undue stresses on the apparatus, while the deepest depth was far enough away from the bottom to avoid inadvertant contact.

D. THE NUC TOWER

The NUC tower is located approximately one mile off Mission Beach, California in 16 meters of water. The apparatus as depicted in Figure III-2 was mounted on the west side of the tower.

33
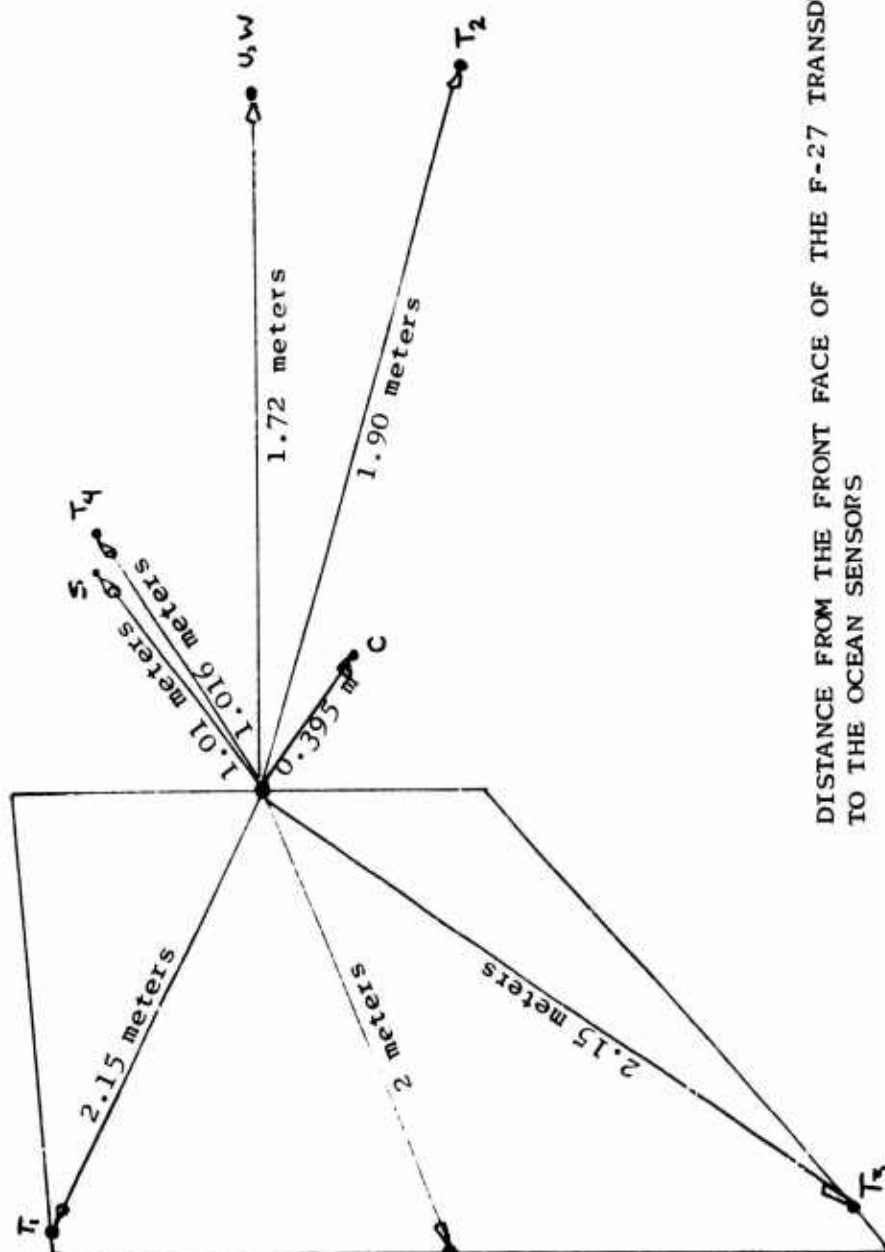
DISTANCE FROM THE FRONT FACE OF THE F-27 TRANSDUCER
TO THE OCEAN SENSORS

Figure III-3

The electronics were installed on the main deck, while the appa-
ratus was handled from the second deck immediately below. (See
Figure III-4.)

Environmental factors were observed at the tower while the
runs were in progress. The factors noted were:

1. swell: from the northwest, two feet from crest to
trough, with an estimated period of four to five seconds.

2. wind: 310°, 300°, 320° from 9 knots to 7.5 knots during
the course of the experiment

3. wind waves six inches from crest to trough

4. some bubbles visible on the surface

E. UNUSUAL EFFECTS

Unusual effects were those effects arising from considerations
other than physical parameters and naturally occurring bubble
populations. All the unusual effects noted were due to animal and
plant life in and around the apparatus during each run.

The area around the tower supported a large population of
small fish ranging up to eight inches in length. It was noted
that fish were attracted to the apparatus when it was lowered
initially, but resumed their normal habits after a short period
of time. Fish could not affect the wire mounted hydrophone, nor
were any effects noted, since fish swimming through the sound beam
would affect the modulation for a minimal amount of time.

Plant life could affect the equipment by drifting into it.
There was a small amount of kelp in the area at all depths, but
no acoustic effects noted during the runs.
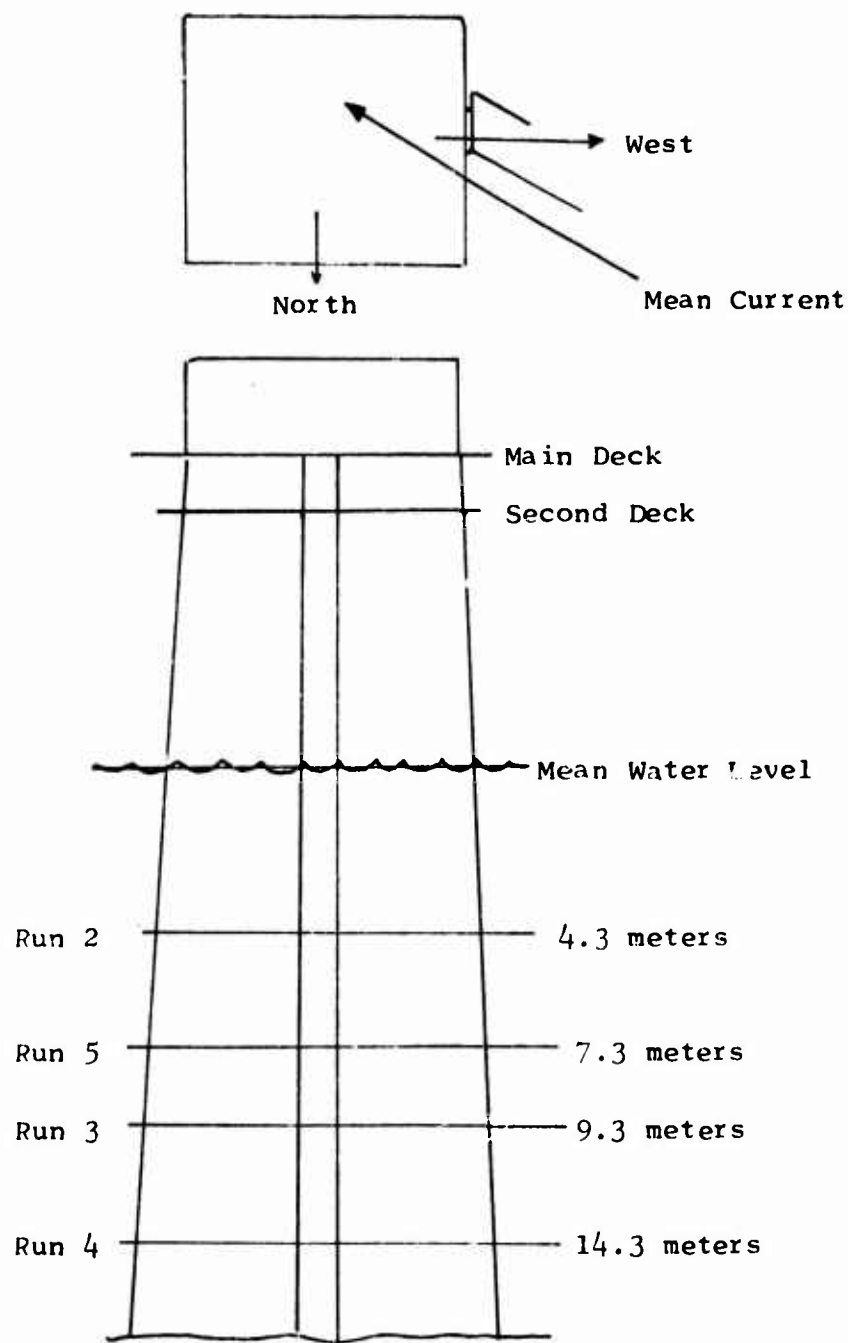
THE NUC TOWER: DEPTHS OF EACH RUN,
AND ORIENTATION

Figure III-4

Boat traffic around the tower had some effect, and could have been sources of turbulent velocity and bubbles which could noticibly affect the amplitude modulation of the acoustic signal. This effect was quite apparent during the Run 5, when there was a boat idling in the area.

F. ORGANIZATION OF INDIVIDUAL RUNS

All information from each sensor was recorded on Sangamo Model 3500 tape recorder. Between individual runs, all sensors were monitored for proper output. After a depth change, a few minutes were allowed for all instruments to be checked for proper operation. When all instruments were checked and operating, the tape recorder was started. The simultaneous start and stop times controlled by the tape recorder insured an accurate run period for all sensors.

The recorder channel allocation was as follows:

Channel 1.: Ramsey probe temperature

Channel 2.: Ramsey probe velocimeter

Channel 3.: Bissett-Berman salinometer

Channel 4.: Turbulent velocity (v)

Channel 5.: Turbulent velocity (w)

Channel 6.: Baylor wave height probe

Channel 7.: Amplitude modulation

Channel 8.: Pressure wave height probe

Channel 9.: Thermistor T_1

Channel 10.: Bissett-Berman temperature

Channel 11.: Thermistor T_2

Channel 12.: Thermistor T_3

Channel 13.: Phase modulation

Channel 14.: Voice

38

IV. ANALYSIS OF ACOUSTIC RESULTS

A. INITIAL DATA REDUCTION

1. General

The recorded analog data consisted of four twenty minute runs at varying depths. The dynamic range of the recorded voltage was 0.01 to 1.10 volts. The data reduction scheme involved three steps; transfer of the analog data from magnetic tape to a Brush Mark 200 strip-chart recorder, conversion of the printed analog data to digitized data and computer analysis of the digitized data.

2. Magnetic Tape to Strip-Chart Record

The tape recorded data was originally collected at a tape speed of 1 7/8 inches per second. When replayed for the Brush Mark 200 eight channel strip-chart recorder, the data was played at $7\frac{1}{2}$ inches per second, making the strip-chart data for each run one fourth as long as the real-time runs. This had the effect of compressing a twenty minute run to five minutes of strip-chart readout and increasing the apparent frequencies of modulation by a factor of four. At a strip-chart recorder speed of five milli-meters per second, each printed run was presented on 1.5 meters of chart.

The strip-chart recorder was set to present the data at 50 millivolts per millimeter, or 1.27 volts per inch.

The other seven strip-chart channels were used to visually compare some of the ocean sensor outputs to the output from the amplitude modulation data. The other seven strip-chart channels

were allocated as follows:

      Channel 1.: Salinometer

      Channel 2.: v velocity

      Channel 3.: w velocity

      Channel 4.: Amplitude modulation

      Channel 5.: Baylor wave height

      Channel 6.: Thermistor T_3

      Channel 7.: Bissett-Berman temperature

      Channel 8.: Velocimeter

It was then possible to make preliminary visual comparison of the waveforms of the recorded outputs in order to observe any similarities in the waveforms. (See Figures IV-1 through IV-4.)

3. Strip-Chart Record to Digital Tape

The strip-chart records of each of the four runs to be analyzed were taken to the Fleet Numerical Weather Central facility at Point Piños, California to be recorded as digitized data on magnetic tape. The data were digitized directly from the strip chart recording on the facility's tracing digitizer. The digitizer recorded data points in increments of hundredths of an inch in the y-direction for each one one-hundredth of an inch of travel in the x-direction, and transferred the x and y values to a nine-track magnetic tape.

The digitizing was initiated at the start of each run, visible on the strip-chart as a vertical line produced when the tape recorder run was commenced. The zero amplitude value in the y-direction and the zero time value in the x-direction were taken at this line. There were data excursions in the positive and

40
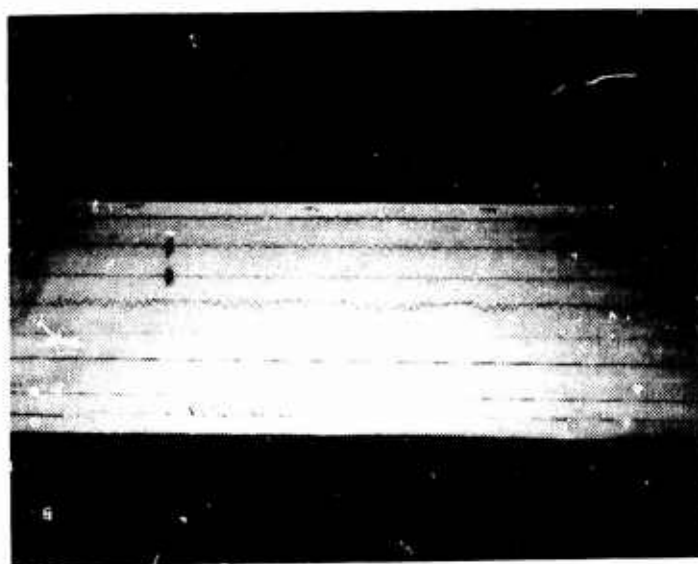
EIGHT CHANNEL BRUSH RECORDER READOUT FOR RUN 2, DEPTH:
4.3 meters. top to bottom: salinometer, v-turbulence,
w-turbulence, amplitude modulation, wave height, ther-
mistor 3, Bissett-Berman temperature and velocimeter
readouts.

Figure IV-1
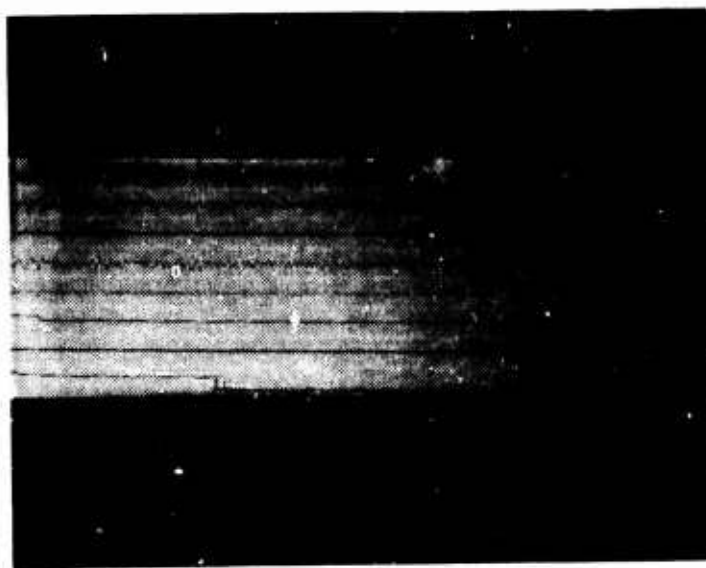
EIGHT CHANNEL BRUSH RECORDER READOUT FOR RUN 5 DEPTH:
7.3 meters. For channel identification, see Fig. IV-1.

Figure IV-2
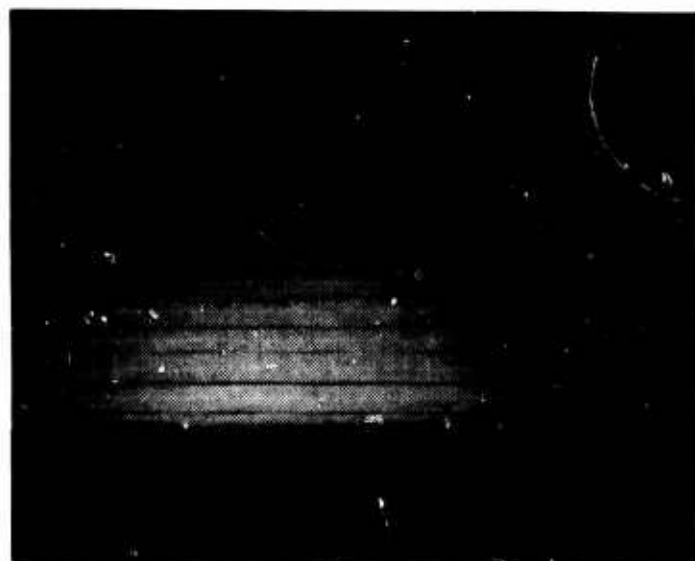
EIGHT CHANNEL BRUSH RECORDER READOUT FOR RUN 3 DEPTH:
9.3 meters. For channel identification, see Fig. IV-1.

Figure IV-3
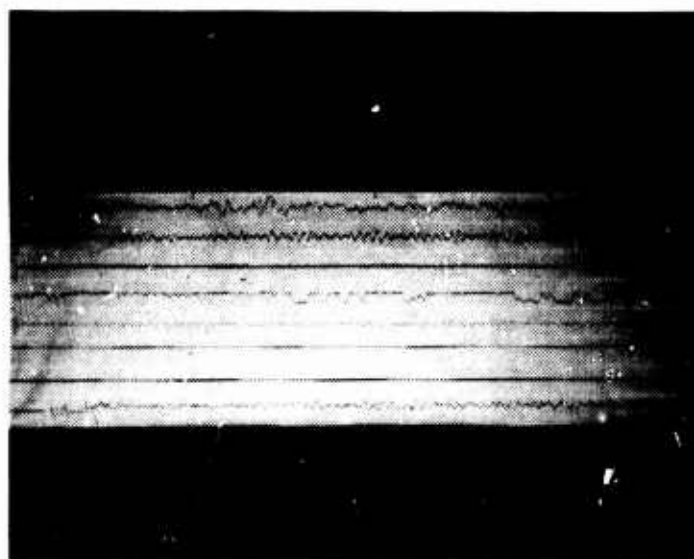
EIGHT CHANNEL BRUSH RECORDER READOUT FOR RUN 4 DEPTH:
14.3 meters. For channel identification see Fig. IV-1.

Figure IV-4

negative directions, measured in one-hundredths. The conversion factors were 0.0127 volts per data point in the y-direction, and 0.01265 seconds (real time) per data point in the x-direction.

4. Digitized Data from Magnetic Tape to IBM Data Cards

The conversion of the digitized data from magnetic tape to data cards for analysis on the IBM 360 digital computer was accomplished in the Fleet Numerical Weather Central's CDC 5000 computer.

The procedure utilized Program I, and converted at least 5600 data points for each run, corresponding to nineteen minutes of real data collection time. This decrease in data time was due to an uncertainty of stopping points on the strip-chart readouts, and allowed an identical number of data points for each run.

B. ANALYSIS OF ACOUSTIC DATA

The data from each run were analyzed on the Naval Postgraduate School's IBM 360 digital computer.

The analyses were performed on time-varying amounts of fractional amplitude modulation. The raw data as presented on data cards was in varying values expressed as positive and negative hundredths of an inch. The conversion was common to all programs and is described below:

a. Each run was scanned for the maximum positive value.

b. The maximum positive value was subtracted from all other values and converted to 0.0. This level corresponded to the unmodulated amplitude. All data values were now negative values, all less than zero except for the maximum value.

c. Each value was multiplied by a conversion factor consisting
of (-1.27) which converted the data points to positive voltage
values, and (1/6) which made each point a fractional value of the
maximum amplitude of six volts. The resultant data points could
now be expressed as fractional modulation:

$$F = \left[\frac{(\text{unmodulated voltage}) - (\text{modulated voltage})}{(\text{unmodulated voltage})} \right]$$

The converted raw data was then analyzed for the mean,
variance, temporal correlation and power spectral density of each
run in Program II. Program III computed a histogram of the amount
of fractional modulation versus the number of occurrences of each
value. An independent calculation of the mean, mean square and
variance was made in Program IV. (See Figures IV-5 through IV-7.)
The results of the various analyses are presented in the following
section.

DATA ANALYSIS SCHEME: PROGRAM II

```
┌─────────────────────────────┐
│  RAW DATA ON IBM CARDS       │
└─────────────────────────────┘
              │
              ▼
┌─────────────────────────────┐      ┌─────────────────────────────┐
│  FIND MAXIMUM VALUE (XMAX)   │─────▶│  VALUE OF UNMODULATED        │
│    SET EQUAL TO ZERO         │      │  AMPLITUDE = 0.0             │
└─────────────────────────────┘      └─────────────────────────────┘
              │
              ▼
┌─────────────────────────────┐      ┌─────────────────────────────┐
│  SUBTRACT ALL VALUES FROM    │─────▶│  (NEGATIVE) VALUES OF XMAX   │
│  MAX VALUE (Xi -XMAX)        │      │  LESS EACH MODULATED VALUE   │
└─────────────────────────────┘      └─────────────────────────────┘
              │
              ▼
┌─────────────────────────────┐      ┌─────────────────────────────┐
│  MULTIPLY VALUES BY (-1.27)  │─────▶│  CONVERTS ALL VALUES TO      │
│                              │      │  POSITIVE VOLTAGE DIFFERENCE │
└─────────────────────────────┘      └─────────────────────────────┘
              │
              ▼
┌─────────────────────────────┐      ┌─────────────────────────────┐
│  DIVIDE ALL VALUES BY (6.0)  │─────▶│  CONVERTS ALL VALUES TO PER- │
│                              │      │  CENT MODULATION             │
└─────────────────────────────┘      └─────────────────────────────┘
```
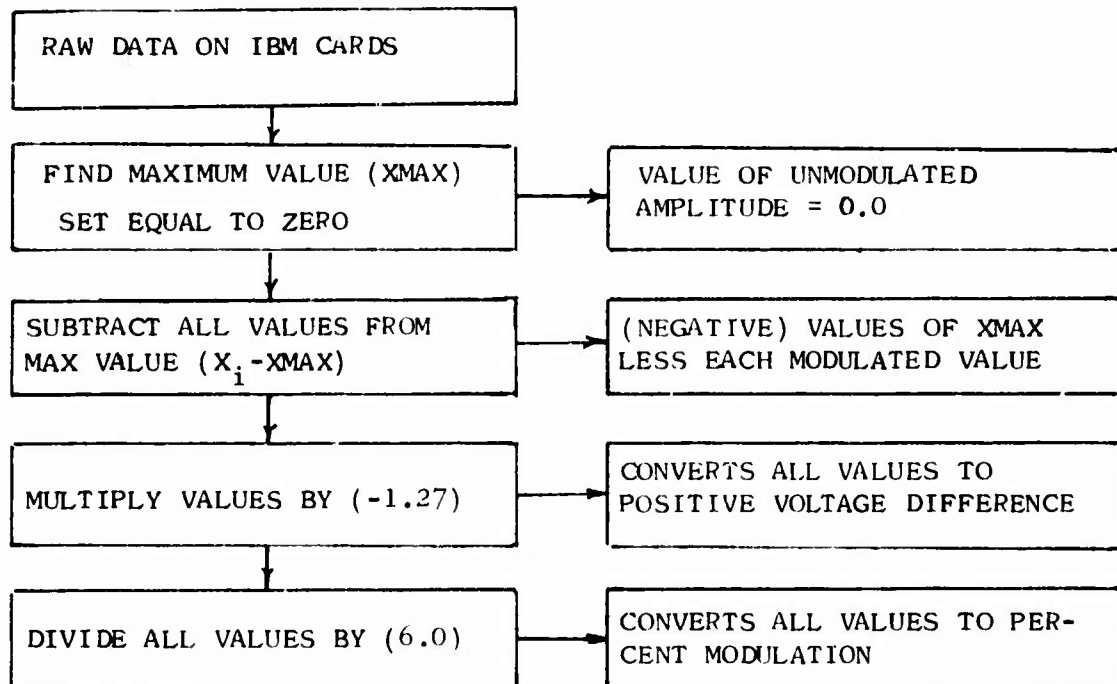
AT THIS POINT, ALL VALUES MAY BE EXPRESSED AS:

$$F = \left[\frac{(\text{UNMODULATED VOLTAGE}) - (\text{MODULATED VOLTAGE})}{(\text{UNMODULATED VOLTAGE})} \right]$$

```
┌─────────────────────────────┐      ┌─────────────────────────────┐
│  FIND MEAN VALUE             │─────▶│  ⟨ (VMAX - VMOD)/VMAX ⟩       │
└─────────────────────────────┘      └─────────────────────────────┘
              │
              ▼
┌─────────────────────────────┐      ┌─────────────────────────────┐
│  FIND VARIANCE               │─────▶│  σ² = ∫ E(F) dF              │
└─────────────────────────────┘      └─────────────────────────────┘
              │
              ▼
┌─────────────────────────────┐      ┌─────────────────────────────┐
│  FIND TEMPORAL CORRELATION   │─────▶│  C(τ) = lim ...              │
└─────────────────────────────┘      └─────────────────────────────┘
              │
              ▼
┌─────────────────────────────┐      ┌─────────────────────────────┐
│  FIND POWER SPECTRAL DENSITY │─────▶│  E(F) = ℱ[C(τ)]             │
└─────────────────────────────┘      └─────────────────────────────┘
```

$$\left\langle \frac{\text{VMAX} - \text{VMOD}}{\text{VMAX}} \right\rangle$$

$$\sigma^2 = \int E(F)\, dF$$

$$C(\tau) = \lim_{T \to \infty} \frac{1}{T} \int_{-T/2}^{T/2} F(t)\, F(t+\tau)\, dt$$

$$E(F) = \mathcal{F}\left[C(\tau) \right]$$

Figure IV-5

45

DATA ANALYSIS SCHEME: PROGRAM III


```
┌─────────────────────────────────────────────┐
│                                             │
│           RAW DATA ON IBM CARDS             │
│                                             │
└─────────────────────────────────────────────┘
                     │
                     ▼
┌─────────────────────────────────────────────┐
│        CONVERSION OF ALL DATA VALUES        │
│       TO FRACTIONAL MODULATION VALUES       │
│                                             │
└─────────────────────────────────────────────┘
                     │
                     ▼
┌─────────────────────────────────────────────┐
│     ESTABLISH "BINS" FROM 0.0 TO 0.170      │
│   IN STEPS OF 0.001, YIELDING 171 "BINS"    │
│        (0.160 IS THE MAXIMUM VALUE OF       │
│          FRACTIONAL MODULATION)             │
│                                             │
└─────────────────────────────────────────────┘
                     │
                     ▼
┌─────────────────────────────────────────────┐
│   SCAN EACH VALUE OF FRACTIONAL MODULATION  │
│      AND PLACE IN THE APPROPRIATE BIN       │
│                                             │
└─────────────────────────────────────────────┘
                     │
                     ▼
┌─────────────────────────────────────────────┐
│   COUNT THE NUMBER OF OCCURENCES IN EACH BEN │
│                                             │
└─────────────────────────────────────────────┘
```

Figure IV-6

Figure IV-7

V. ACOUSTIC RESULTS

A THE STRIP-CHART READOUTS

Figures V-1 through V-4 are representative 168-second portions of each twenty-minute run. The variation in voltage from peak-to-peak is approximately one volt, and the apparent frequencies of variation are four times the actual frequencies occurring during each run.

From visual inspection of the strip-charts, it may be seen that the modulations occurring during the two shallow runs (4.3 and 7.3 meters) were more active in frequency than during the two deeper runs (9.3 and 14.3 m.). It must be noted that the 7.3 meter run was conducted after the other runs, and that during most of the period a fifty-foot motor launch was in the area of the tower with with propellors turning. The launch served as a bubble injection device as well as a turbulence generator. The run was not invalidated because the modulation effect of bubbles artificially generated during this run could be compared with that of the ambient medium of the previous runs.

B. MEANS AND VARIANCES

The mean and variance of the amplitude modulation for each run was determined by Computer Run IV. The formulation was based on the fractional modulation F, and was calculated as shown:

$$F = \left[\frac{VMAX - VMOD}{VMAX} \right]$$

48
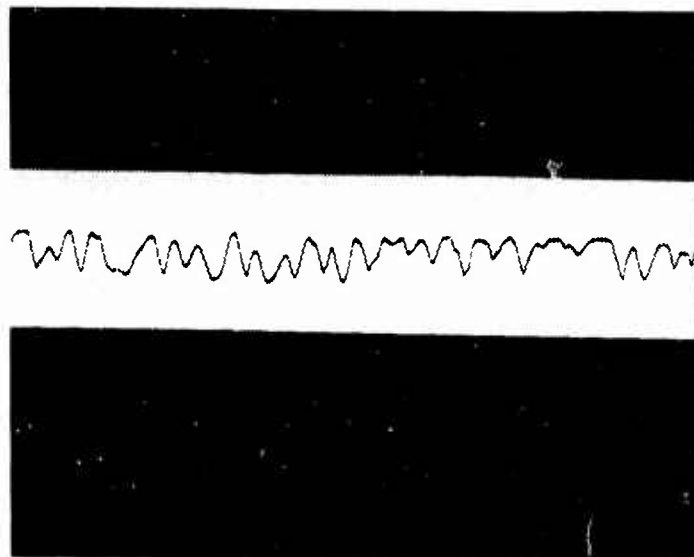
BRUSH RECORDER READOUT OF AMPLITUDE MODULATION RUN TWO DEPTH: 4.3 meters. vertical lines indicate four seconds in real time, horizontal lines indicate 0.25 volts.

Figure V-1
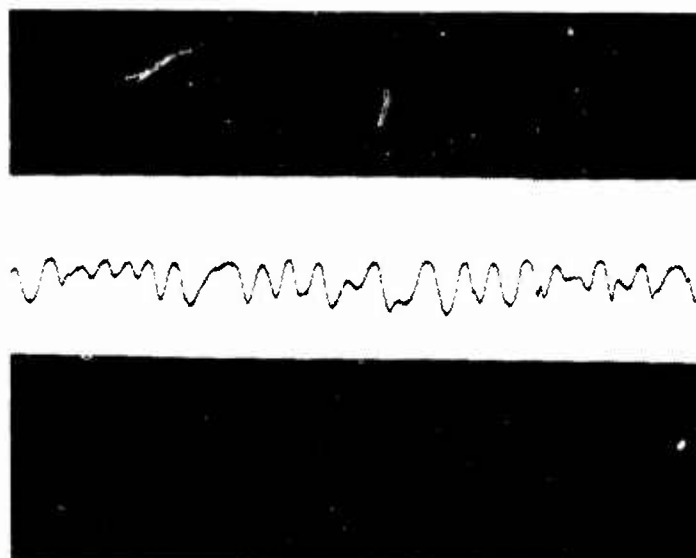
BRUSH RECORDER READOUT OF AMPLITUDE MODULATION RUN 5 DEPTH: 7.3 meters. see caption for Fig. V-1.

Figure V-2

BRUSH RECORDER READOUT OF AMPLITUDE MODULATION RUN 3 DEPTH: 9.3 meters. see caption for Fig. V-1.

Figure V-3
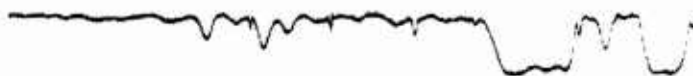
BRUSH RECORDER READOUT FOR AMPLITUDE MODULATION RUN 4 DEPTH: 14.3 meters. see caption for Fig. V-1.

Figure V-4

which resulted in the time series F(t); then,

$$\langle F(t) \rangle = \frac{\sum F_i}{n}$$

where $n = 5600$

and

$$\langle F^2(t) \rangle = \frac{\sum (F_i)^2}{n}$$

and

$$\sigma^2 = \left\{ \langle F^2(t) \rangle - \langle F(t) \rangle^2 \right\}$$

The results obtained from each run were compared with the results of Computer Run II, which determined the mean, temporal correlation and the power spectral density for each run. Effectively, for Program II the mean, $\langle F(t) \rangle$, was determined as in Program IV so that comparison was superflous.

The variance, σ^2, can be formulated in three ways; first as shown above, secondly as the zero-time temporal correlation value,

$$\sigma^2 = C(\tau) \Big|_{\tau=0} = \lim_{T \to \infty} \frac{1}{T} \int_{-T/2}^{T/2} F(t) F(t+\tau) \, dt$$

and thirdly as the value of the area under the curve for the power spectral density:

$$\sigma^2 = \int E(F) \, dF$$

It should be noticed that at all depths, the three values of the variance are quite close. The slightly different values of σ^2 from the calculation for $C(0)$ and from the simple sorting calculation (Program IV) are solely due to round off error for the latter calculation.

The value of σ^2 derived from the integral of the power spectral density has the largest numerical value. This is the result of limiting the higher frequencies from the calculation of the Fourier pass band, resulting in a rounded "window". This rounding off resulted in a very slightly larger area under the power spectral density curve than would otherwise occur.

The results for each run are shown below:

Run 2: 4.3 meters

Program IV: $\langle F \rangle = 0.0526$

$$\langle F^2 \rangle = 0.0041$$

$$\sigma^2 = 0.0013$$

Program II: $\langle F \rangle = 0.05261$

$$\sigma^2 = C(0) = 0.00131$$

$$\sigma^2 = \int E(F)dF = 0.0014469$$

Run 5: 7.3 meters

Program IV: $\langle F \rangle = 0.0460$

$$\langle F^2 \rangle = 0.0031$$

$$\sigma^2 = 0.0010$$

Program II: $\langle F \rangle = 0.04604$

$$\sigma^2 = C(0) = 0.00096$$

$$\sigma^2 = \int E(F)dF = 0.0009756$$

Run 3: 9.3 meters

Program IV: $\langle F \rangle = 0.0303$

$$\langle F^2 \rangle = 0.0016$$

$$\sigma^2 = 0.0007$$

Program II: $\langle F \rangle = 0.03026$

$$\sigma^2 = C(0) = 0.00067$$

$$\sigma^2 = \int E(F)dF = 0.0007378$$

Run 4: 14.3 meters

Program IV: $\langle F \rangle = 0.0470$

$\langle F^2 \rangle = 0.0040$

$\sigma^2 = 0.0018$

Program II: $\langle F \rangle = 0.0472$

$\sigma^2 = C(0) = 0.00173$

$\sigma^2 = \int E(F)dF = 0.0019268$

The probability density of fractional modulation values for each run is shown on the histograms. (Figures V-5 through V-7.) Although the mean values calculated above do not differ in any orderly manner with depths, the histograms (as well as Figures V-1,2,3 and 4) show that for the shallow depths there are greater numbers of short duration, high modulation values, whereas for the greater depths, the distribution of fractional modulation centers heavily about the lower values. The bimodal P.D.F. at the greatest depth (14.3 meters) shows that onset of infrequent occurrences of very high modulation values. This is the statistical representation of the type of modulation observed on Figure V-4, where the modulation assumes a high value and varies about that value for relatively long periods. The data thereby suggest that as depth is increased the magnitude of the medium inhomogenieties increase and the size (temporal extent) of the inhomogeneous volumes becomes greater as well.

C. TEMPORAL CORRELATION

The temporal correlations (time autocorrelations) for each run are shown on Figures V-8 through V-11. The times to 50%
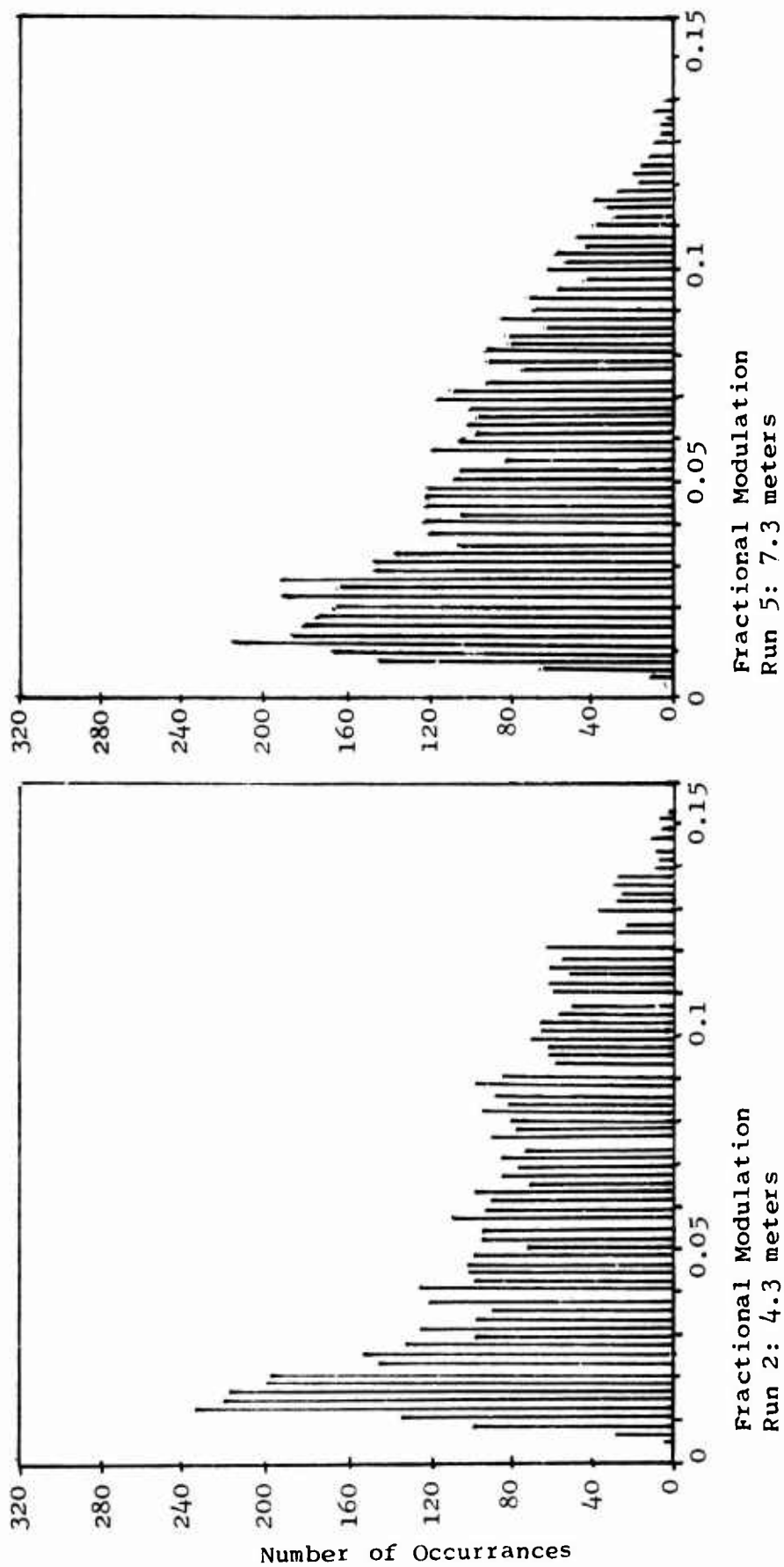
DISTRIBUTION OF FRACTIONAL MODULATION

Figure V-5

DISTRIBUTION OF FRACTIONAL MODULATION
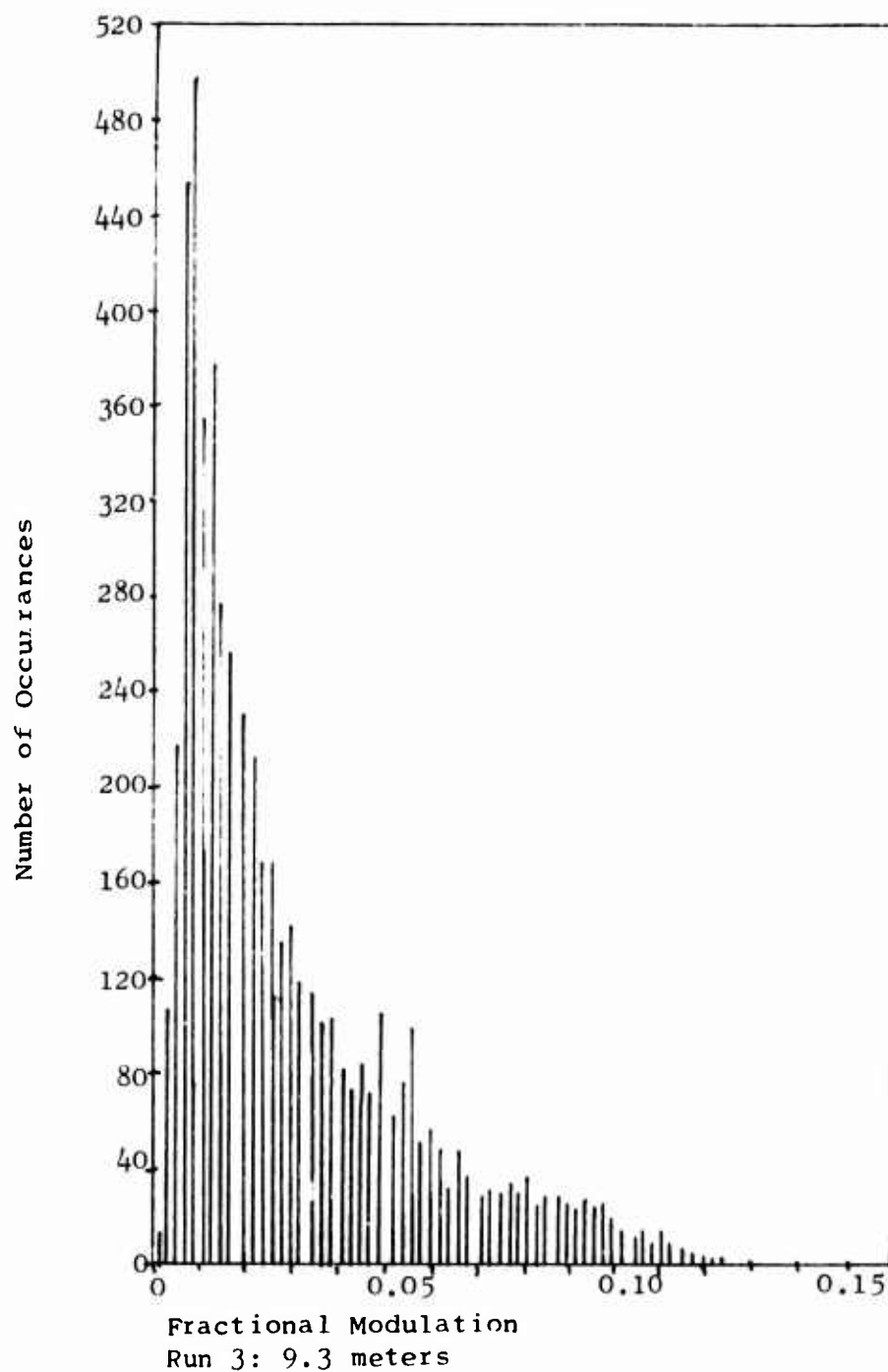
Figure V-6

Fractional Modulation
Run 4: 14.3 meters
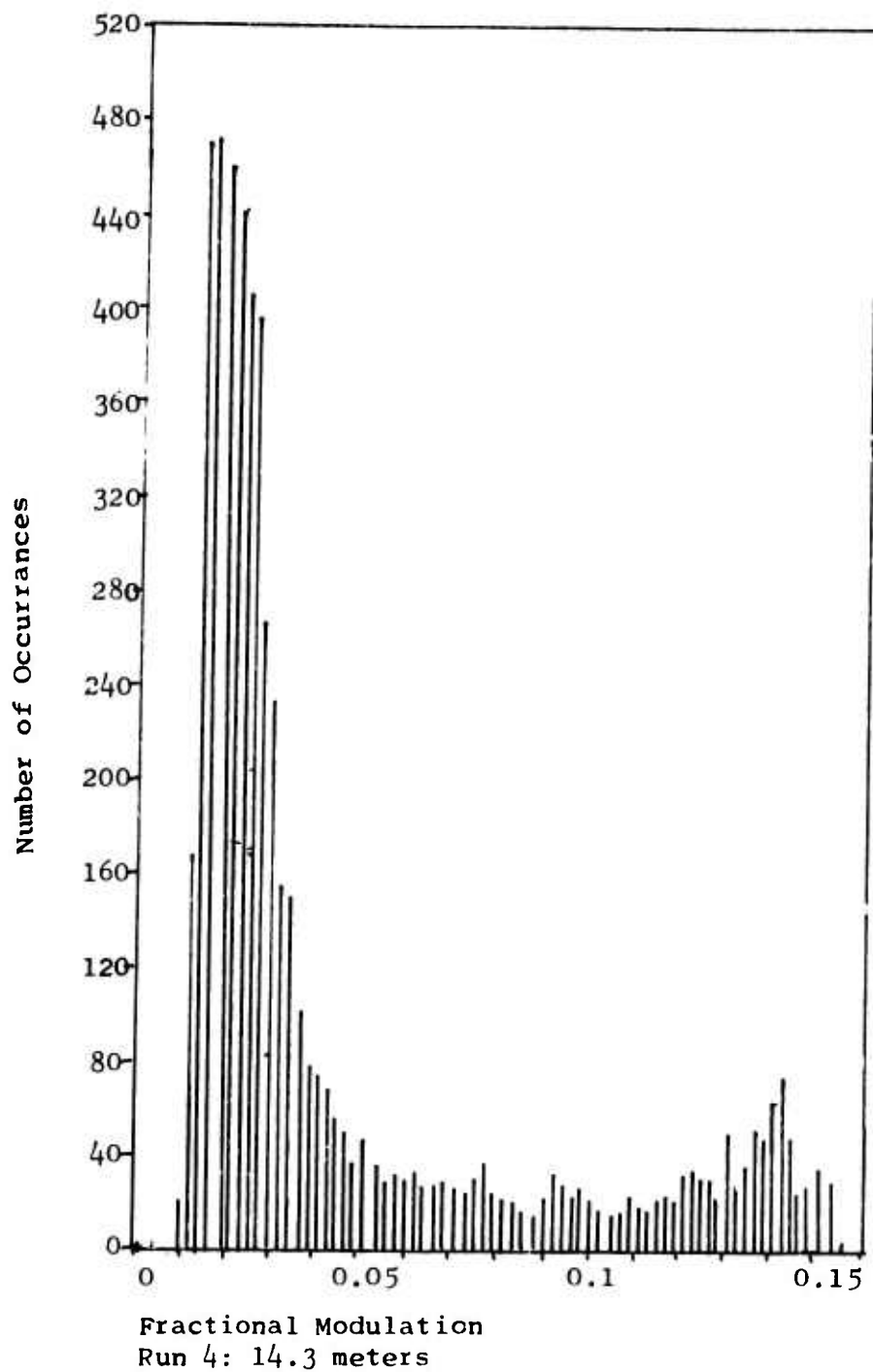
DISTPIBUTION OF FRACTIONAL MODULATION

Figure V-7
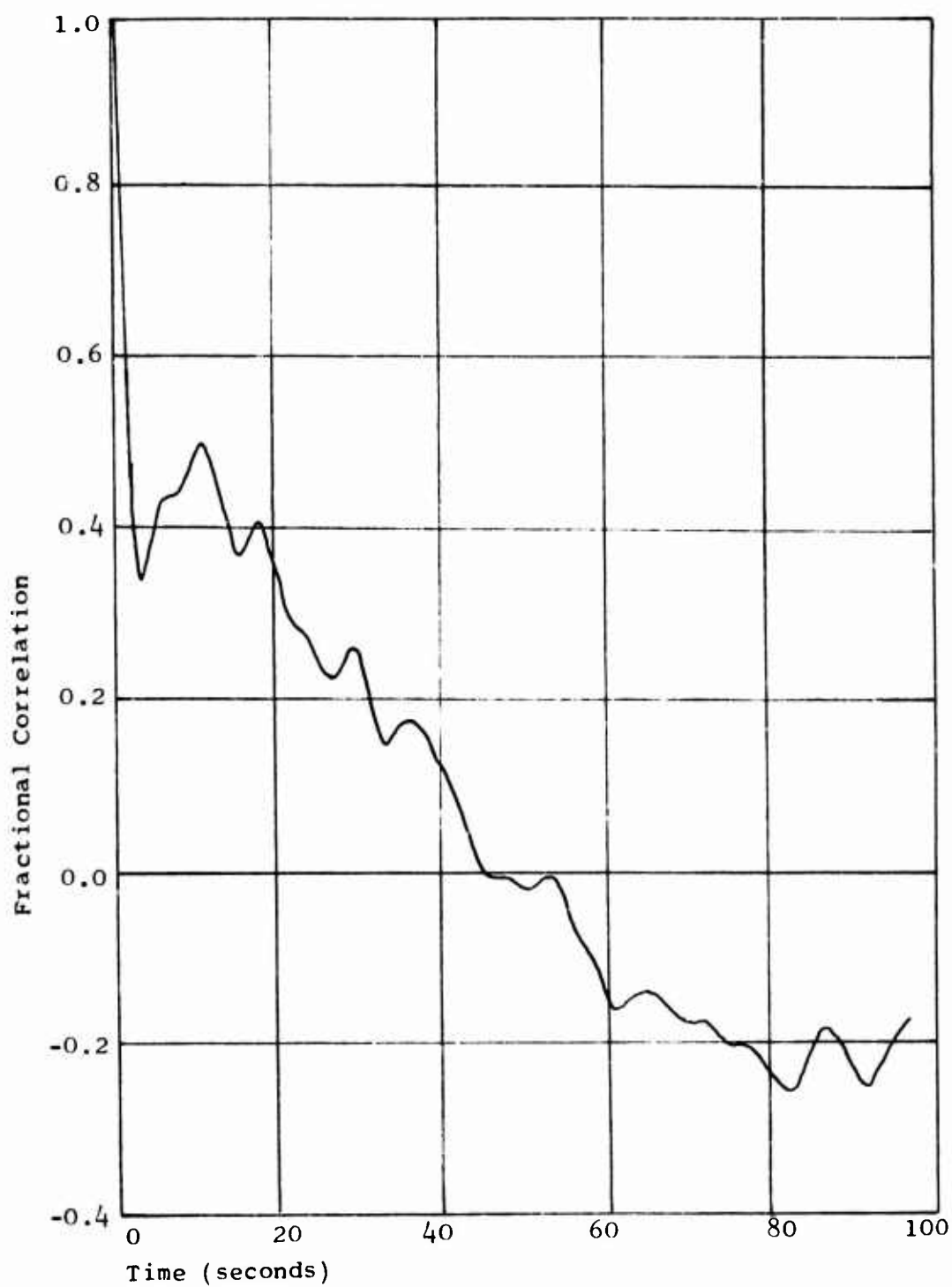
NORMALIZED TEMPORAL CORRELATION OF RUN 2
DEPTH: 4.3 meters

Figure V-8
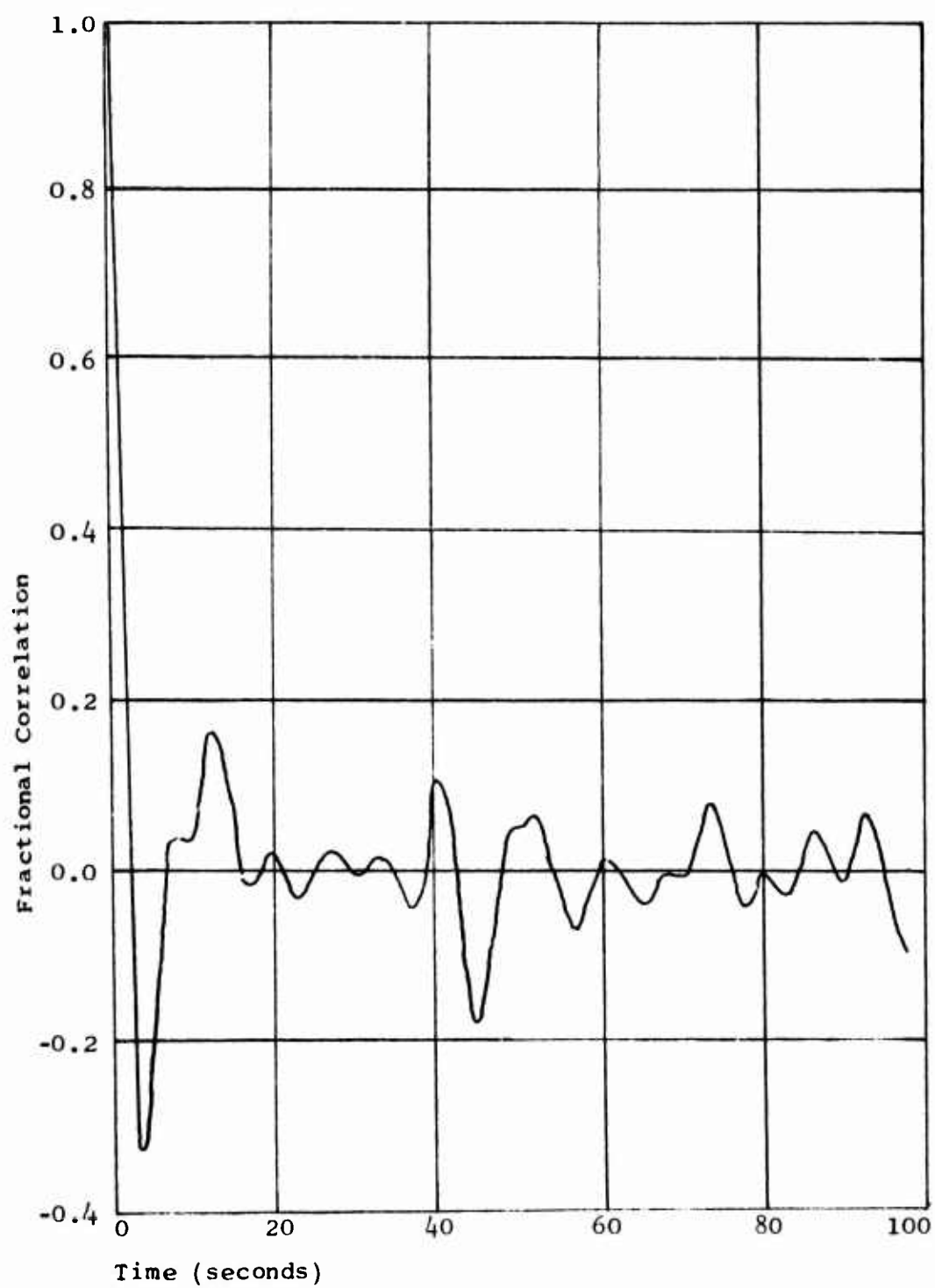
NORMALIZED TEMPORAL CORRELATION OF RUN 5
DEPTH: 7.3 meters

Figure V-9

58
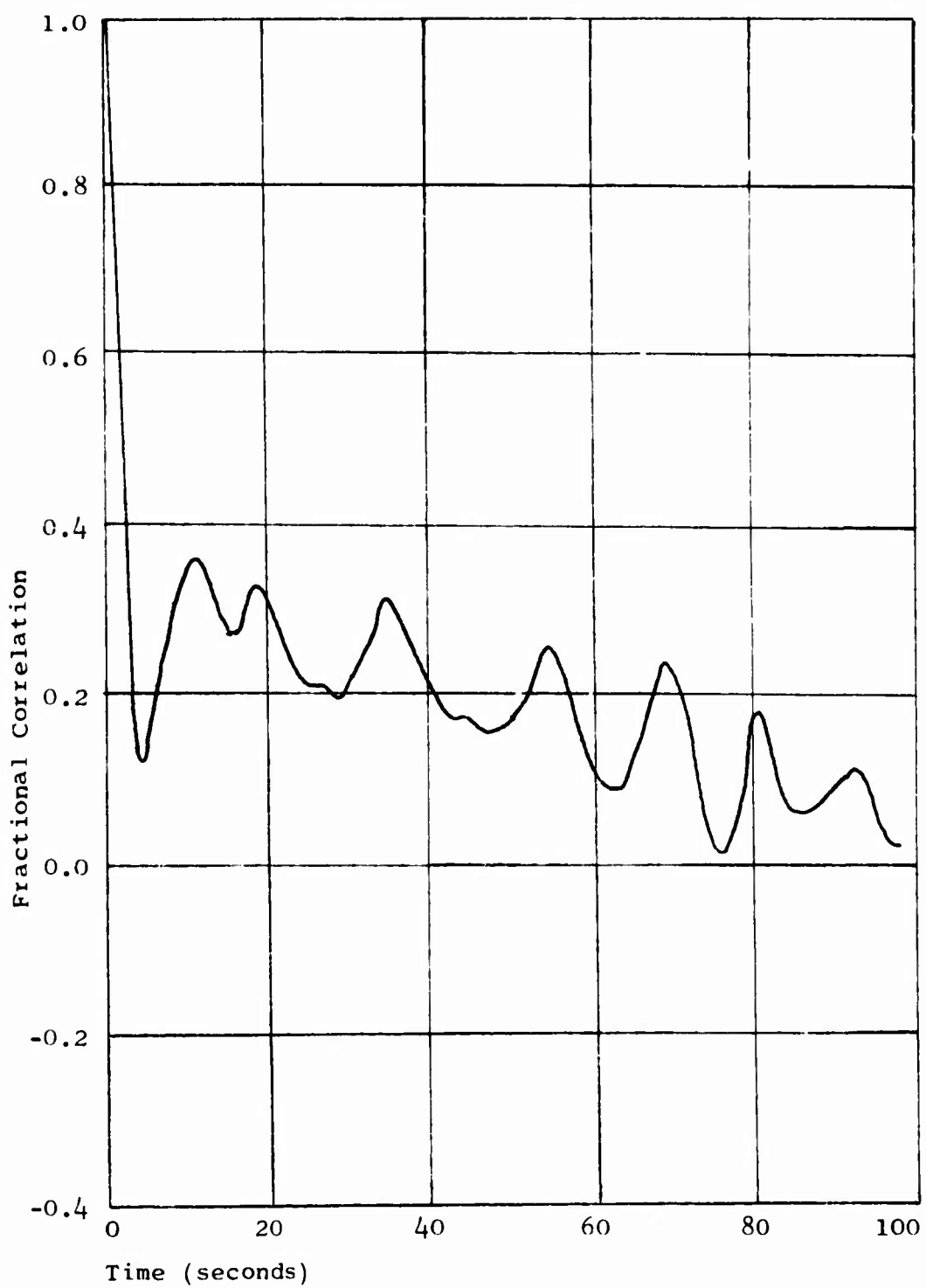
NORMALIZED TEMPORAL CORRELATION OF RUN 3
DEPTH: 9.3 meters

Figure V-10

59
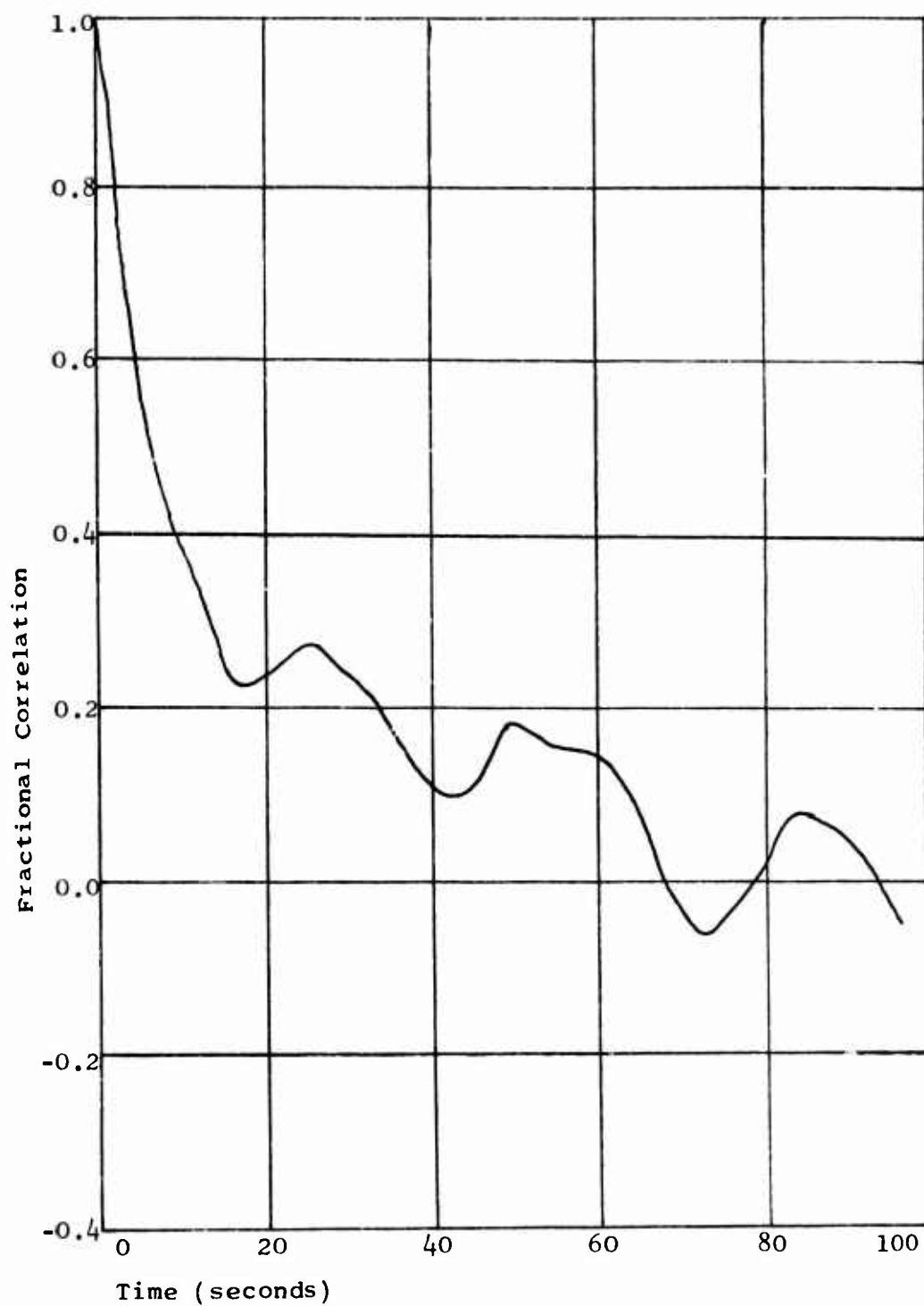
NORMALIZED TEMPORAL CORRELATION OF RUN 4
DEPTH: 14.3 meters

Figure V-11

60

correlation and l/e correlation are shown below:

	Depth (meters)	Time (seconds)
Time to 50%:	4.3	2.33
	7.3	1.43
	9.3	2.23
	14.3	6.9
Time to l/e:	4.3	3.25
	7.3	1.65
	9.3	2.73
	14.3	11.75

It can be seen from the figures that there is a rapid initial decorrelation down to low as 10% for depths of 4.3 and 9.3 meters, and a slower decorrelation for the 14.3 meter depth. All of these runs show a fluctuation between steadily decreasing minima and maxima with a delayed zero crossing. Whitmarsh, Skudrzyk and Urick (1957) hypothesized that such fluctuation was an indication of the size of the inhomogeneous "patches" around the receiver. If Whitmarsh, Skudrzyk and Urick's hypothesis is correct, then the apparent "patch" sizes show an increase with depth. If this is the case, then small-scale turbulence may tend to dominate at all depths near the surface.

The temporal correlation of the 7.3 meter depth is of interest since it is known that an artificially derived bubble and turbulence field was introduced into the volume under consideration. The 7.3 meter depth shows the most rapid decorrelation to zero of all runs, and twice as frequent fluctuations about zero as for the undisturbed

61

water at other depths. This suggests that the ambient "patches" of water were chopped into smaller patches by the boat's propellor.

Another hypothesis might be that the inhomogeneous volumes are more or less "frozen" and that the spatial displacement of these volumes about the acoustic axis may cause the appearance of temporal variation. Corroboration of these hypothetical explanations awaits the complete analysis of the data gathered by the oceanographic sensors.

D. POWER SPECTRAL DENSITY

The power spectral densities (PSD) of each run are plotted against frequency on Figures V-12 through V-15. The power spectral densities show the highest values at those frequencies (0.08 to 0.12 Hz) which appear to correspond with the observed ocean swell frequencies prevailing during each run.

The PSD's show a diminishing value both with increasing frequency and with increasing depth. The two shallowest depths (4.3 and 7.3 meters) show a similarity in the values of PSD from 0 to 1.0 Hz, except for a high "DC" value in the plot for 4.3 meters, resulting in a higher contribution to the integrated value of PSD (σ^2) at that depth. A similar likeness is apparent between the two greater depths (9.3 and 14.3 meters). For frequencies greater than 0.1 Hz, the PSD at the two shallower depths appear to be consistently four to five db greater than for the deeper depths.

The frequencies of relative maxima along each of the PSD curves show similarities at each end of the spectrum. At the low frequency end, the ocean swell frequencies are more pronounced at
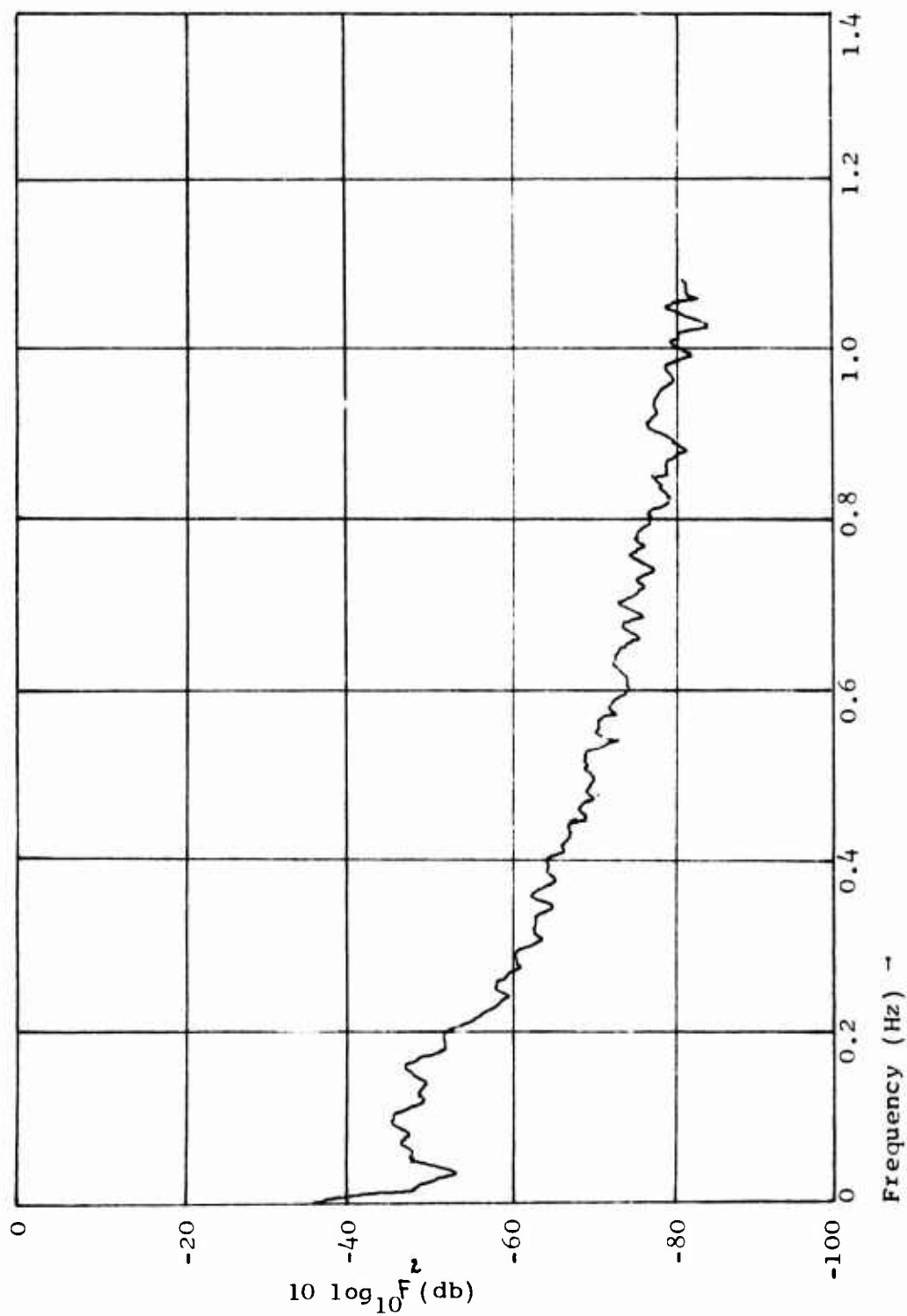
POWER SPECTRAL DENSITY OF RUN 2   DEPTH: 4.3 meters

Figure V-12

63

Frequency (Hz) →

$10 \log_{10} F^2$ (db)
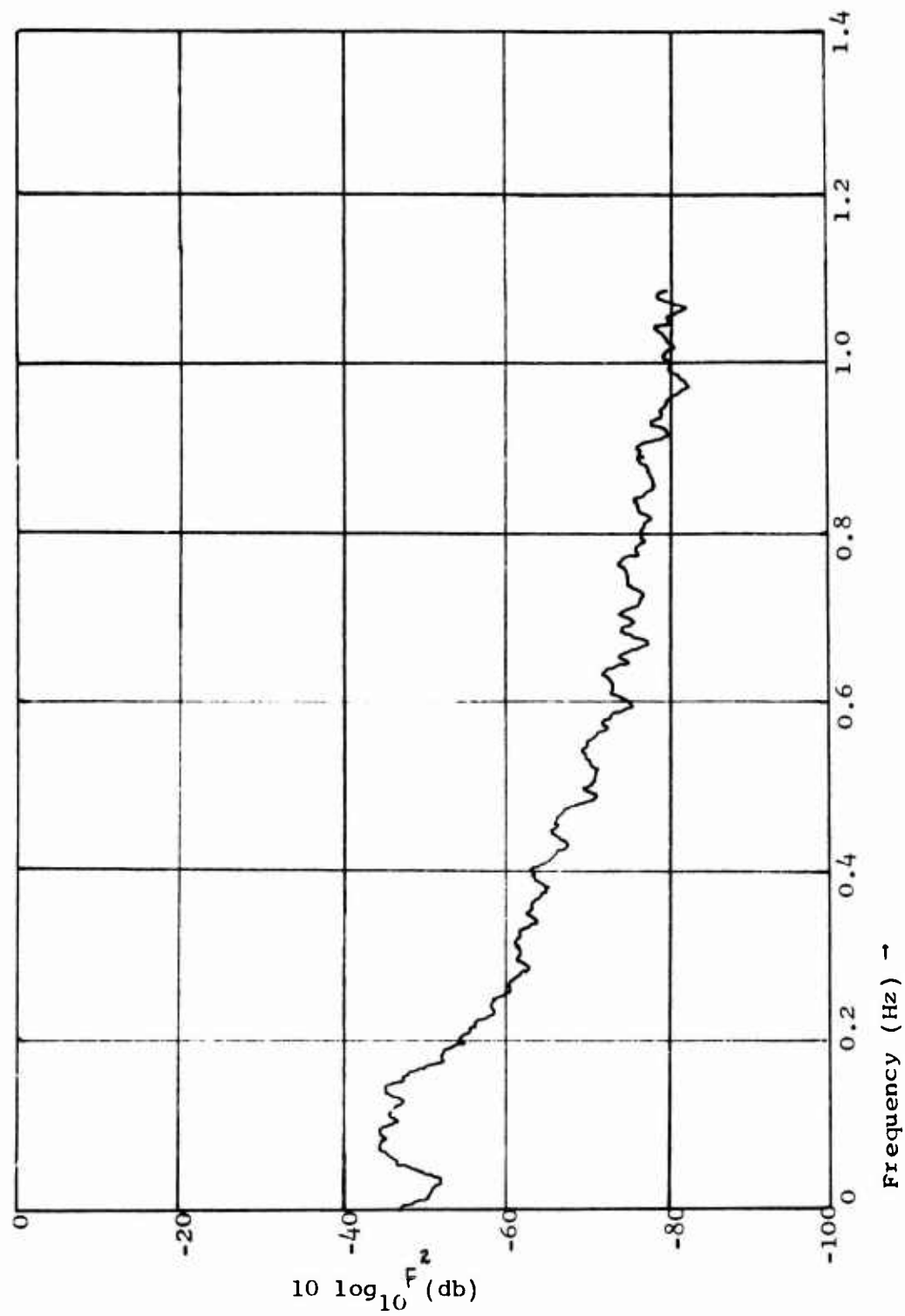
POWER SPECTRAL DENSITY OF RUN 5   DEPTH: 7.3 meters

Figure V-13
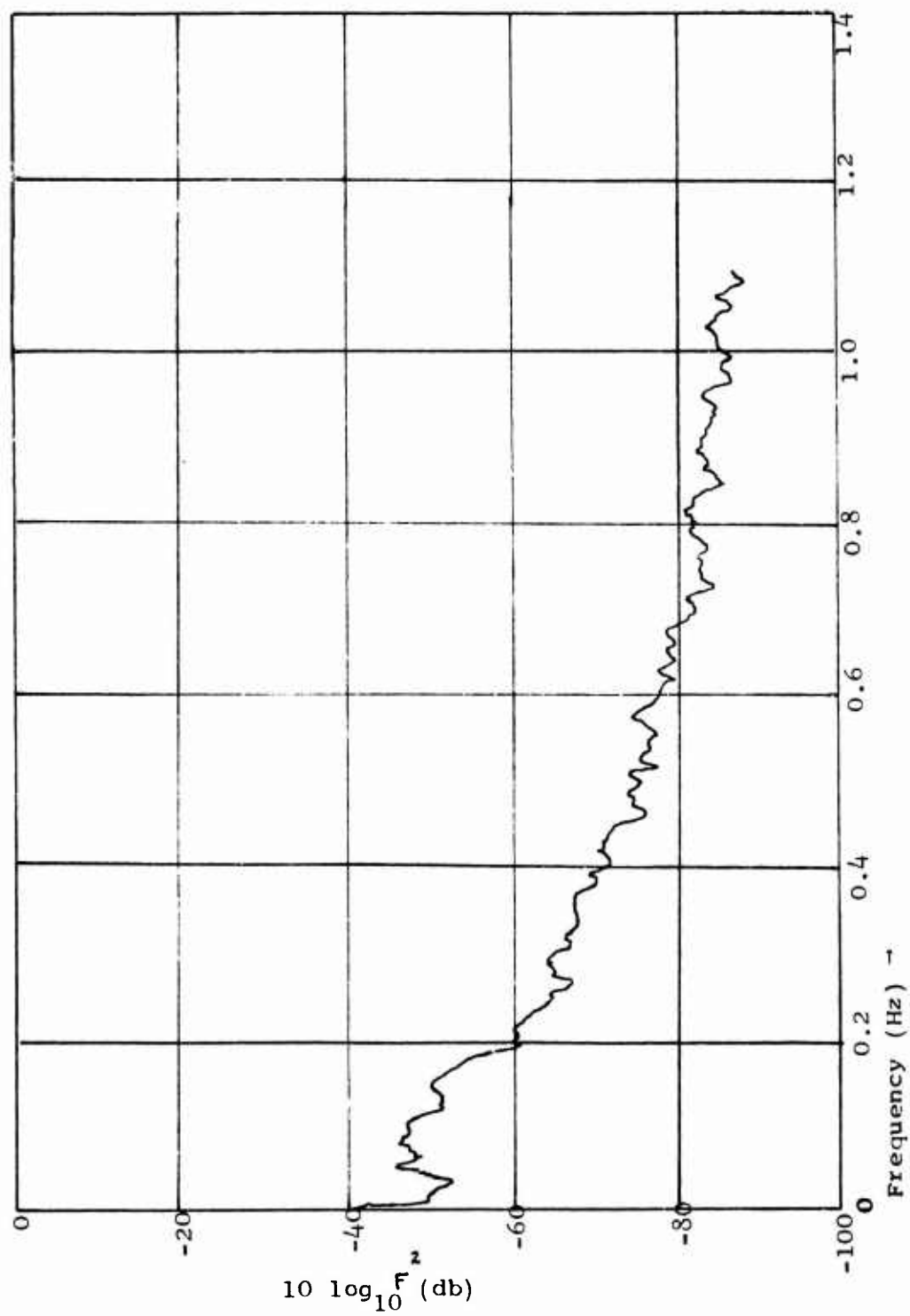
POWER SPECTRAL DENSITY OF RUN 3   DEPTH: 9.3 meters

Figure V-14
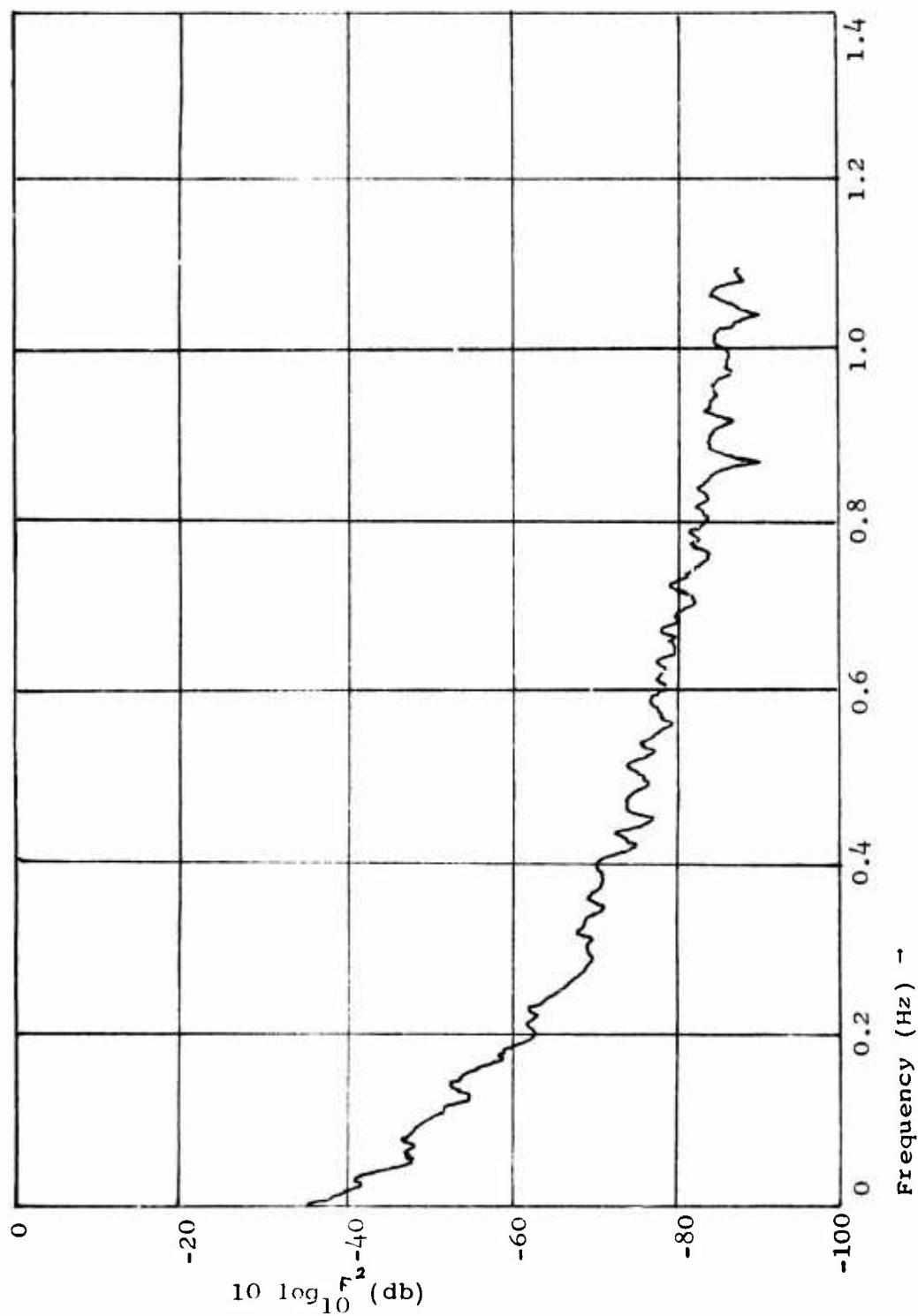
POWER SPECTRAL DENSITY OF RUN 4   DEPTH: 14.3 meters

Figure V-15

Frequency (Hz) →

$10 \log_{10} F^2$ (db)

66

the shallower depths of 4.3 and 7.3 meters. These maxima are

higher for the 7.3 meter run than for the 4.3 meter run, which

may again show the effect of the boat in the area injecting

bubbles and turbulence into the medium. At 9.3 and 14.3 meters,

these low frequency maxima tend to dissappear into the overall

curve, showing a decrease of the component of the amplitude modu-

lation due primarily to the turbulent effect of surface waves.

The amplitude modulation at the higher frequencies (0.2 to

1.0 Hz) could be due to spatial distributions of temperature,

salinity or bubbles which are seen as temporal frequencies due to

movement across the acoustic axis.

E. CONCLUSIONS

The conclusions presented here await the additional infor-

mation that the data from the ocean sensors will provide. This

information will be available in the theses of LCDR Duchock and

LT's Seymour and Bordy, to be presented at the Naval Postgraduate

School in March, 1972. The present conclusions are based upon

the acoustic data alone and are listed below:

1. Amplitude modulation near the ocean surface ranged in

value from zero to sixteen per cent. The maximum amplitudes were

not noticably restricted to any one depth, but as depth increased,

the distribution of modulation values tended to center about the

lower values.

2. The temperal correlation curves for the 4.3, 9.3, and 14.3

meter runs indicate that the size of the volumes of inhomogenieties

("cells") increases as the depth is increased. The correlation

67

curve for the 7.3 meter run shows a significant decrease in the size of the volumes, a direct result of having a motor launch in the area injecting turbulence and bubbles into the volume of water under investigation. Thus it may be seen that in the ambient ocean, cells of microstructure are larger at greater depth. Near surface cells would tend to be reduced in size by the action of turbulence arising from the effect of surface waves.

3. A comparison of the variances of the two shallow runs, at 4.3 and 7.3 meters, shows that there is a small difference between the two. $(\sigma^2(4.3) = 0.0013$ and $\sigma^2(7.3) = 0.0010.)$ Comparing the temporal correlations for the two runs it maybe seen that the decorrelation time for the 7.3 meter run is one-half that of the 4.3 meter run, with more numerous fluctuations about the zero axis. Such data suggests a reduction in the size of the cells of inhomogeniety.

Mintzer's formula for the variance of acoustic amplitude modulation, derived for an exponential correlation function (see Appendix I)

$$(CV)^2 \sqrt{\pi} \, k_0^2 \alpha^2 a \, r$$

shows the dependence of variance on the wave number, k, range, r, the RMS variation of the index of refraction, α, and the size of the inhomogenieties, a. In this experiment, wave number and range were constant; since neither σ^2 nor $(CV)^2$ changed appreciably, it can be deduced that there was a simultaneous increase in α (with the reduction of a) for the 7.3 meter run.

4. The parameters which could cause a change in the RMS variation of the index of refraction, α, were temperature and salinity microstructure, and bubbles.

68

The effect of resonant bubbles on the change in α would be very great. Since bubble populations decrease with depth, this might account for the implied decrease in α with depth. When in the presence of a motor launch, the size of the inhomogeneous volumes were made smaller, there was a concurrent increase in the bubble population and in the value of α. The changes and variations in the other parameters, chiefly temperature and salinity, should be accounted for in subsequent analyses, and a quantitative estimate of the relative effect of bubbles on amplitude modulation may be possible.

5. The power spectral densities indicate that most of the modulation takes place at those frequencies corresponding to the frequencies of the surface waves. This effect was noticable down to the greatest depth (14.3 meters) although the prominemce of the PSD's at the surface-wave frequencies tended to disappear with greater depth.

6. In summary, the major causes of acoustic amplitude modulation at 60 kHz in this near-surface volume of ocean could well have been the effects of mobile, random bubble populations acted upon by particle velocities generated by the action of surface waves.

F. SUGGESTIONS FOR FURTHER EXPERIMENTS

The basic questions left incompletely answered by this investigation are the relative effect of bubbles versus the other causes of amplitude modulation near the surface, and the spatial effect of the inhomogenieties upon the transmission of sound. Later analysis of the oceanographic data will help to answer this question.

It is suggested that further experiments of this kind would be valuable. In order to investigate the spatial effects of the inhomogenieties, the basic apparatus of this experiment could be modified as shown in Figure V-16 in order to attempt some cross-correlation of the amplitude modulation received by each of the hydrophones. In order to more completely investigate the question of transport versus the stationary oscillation of inhomogenieties, more thermistors could be mounted as shown on Figure V-16.

The question of bubbles and bubble populations in an area might be answered either by analysis of all other parameters and their effect, or by deliberately generating bubbles in the volume of water to note their effect on ambient conditions.

Receiving Hydrophones

Acoustic Axis

Thermistors

Transducer

Thermistors
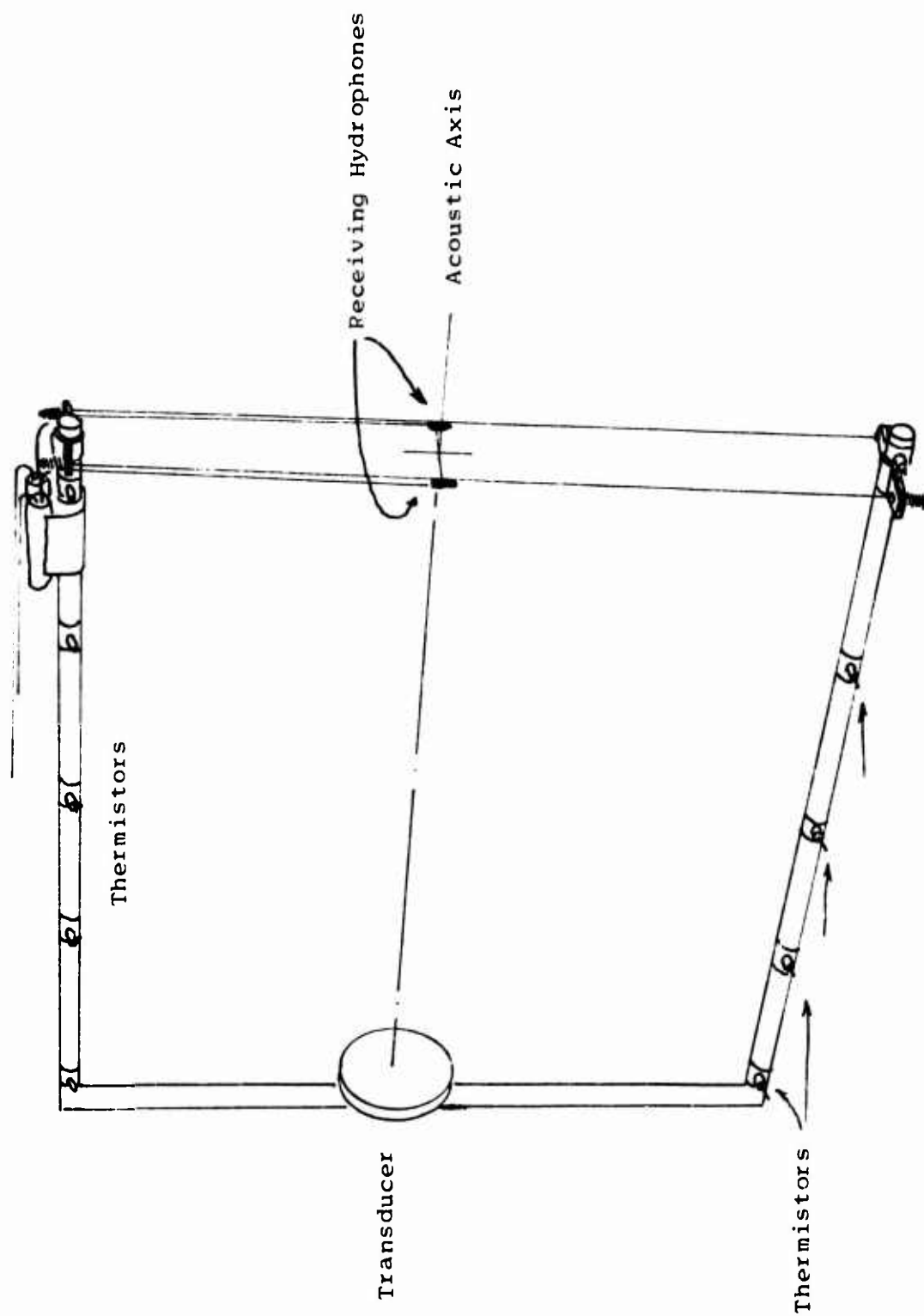
SUGGESTED CONFIGURATION OF THE ACOUSTIC APPARATUS
FOR SPATIAL STUDY

Figure V-16

APPENDIX

THE RELATION BETWEEN F AND CV

The relation between F, the fractional modulation which is used in the development of the experiment, and CV, which Stone and Mintzer call the "coefficient of variation" will be developed.

Fractional modulation is defined in terms of the voltages as shown below:

$$F = \left[\frac{VMAX - V}{VMAX} \right]$$

where V = modulated voltage

VMAX = unmodulated voltage

The coefficient of modulation is defined by Stone and Mintzer in terms of pressure amplitude, P, as shown below:

$$(CV)^2 = \frac{(\langle P^2 \rangle - \langle P \rangle^2)}{\langle P \rangle^2}$$

Then if one assumes that P = KV, or that a constant factor relates the two values, as it does in the equipment used for these experiments, then:

$$(CV)^2 = \frac{(\langle KV \rangle^2 \rangle - \langle KV \rangle^2)}{\langle KV \rangle^2} = \frac{K^2}{K^2} \left[\frac{\langle V^2 \rangle - \langle V \rangle^2}{\langle V \rangle^2} \right]$$

Fractional modulation was used in this experiment because small fluctuations were anticipated. A development between the variance of the fractional modulation and the term $(CV)^2$ is shown below:

$$F = \left[\frac{VMAX - V}{VMAX} \right] = \left(1 - \frac{V}{VMAX} \right)$$

72

$$\sigma^2 = \left[\langle F^2 \rangle - \langle F \rangle^2 \right]$$

$$\sigma^2 = \left\langle \left(1 - \frac{V}{V_{MAX}} \right)^2 \right\rangle - \left\langle 1 - \frac{V}{V_{MAX}} \right\rangle^2$$

$$\sigma^2 = \left\langle 1 - 2\frac{V}{V_{MAX}} + \left(\frac{V}{V_{MAX}} \right)^2 \right\rangle - \left(\langle 1 \rangle - \left\langle \frac{V}{V_{MAX}} \right\rangle \right)^2$$

$$\sigma^2 = \langle 1 \rangle - 2\left\langle \frac{V}{V_{MAX}} \right\rangle + \left\langle \left(\frac{V}{V_{MAX}} \right)^2 \right\rangle - \langle 1 \rangle + 2\left\langle \frac{V}{V_{MAX}} \right\rangle - \left\langle \frac{V}{V_{MAX}} \right\rangle^2$$

$$\sigma^2 = \left\langle \left(\frac{V}{V_{MAX}} \right)^2 \right\rangle - \left\langle \frac{V}{V_{MAX}} \right\rangle^2$$

or, since V_{MAX} is a constant,

$$\sigma^2 = \frac{1}{(V_{MAX})^2} \left[\langle V^2 \rangle - \langle V \rangle^2 \right]$$

multiplied by the factor $\dfrac{\langle V \rangle^2}{\langle V \rangle^2}$ the variance may now be expressed:

$$\sigma^2 = \frac{\langle V \rangle^2}{(V_{MAX})^2} \left[\frac{\langle V^2 \rangle - \langle V \rangle^2}{\langle V \rangle^2} \right]$$

Where the second term is a numerical value multiplied by Mintzer and Stones' expression for the coefficient of variation.

The value multiplied against the coefficient of variation is

$$\frac{\langle V \rangle^2}{(V_{MAX})^2}$$

which is numerically obtainable as follows:

$$\langle F \rangle = 1 - \langle V \rangle$$

$$\therefore \quad \langle V \rangle = 1 - \langle F \rangle$$

for all runs, the value of V_{MAX} was 6 volts.

$$\therefore \quad \frac{\langle V \rangle^2}{(V_{MAX})^2} = \frac{(1 - \langle F \rangle)^2}{36}$$

73

The relation between σ^2 and $(CV)^2$ will be calculated for the 4.3 meter run:

$$\frac{\langle v \rangle^2}{(V_{MAX})^2} = \frac{(1 - 0.0526)^2}{36} = \frac{(0.9474)^2}{36} = 0.02496$$

and in the 7.3 meter run was:

$$\frac{\langle v \rangle^2}{(V_{MAX})^2} = \frac{(1 - 0.0460)^2}{36} = \frac{(0.9540)^2}{36} = 0.02530$$

It is noted that the conversion factor does not significantly change with depth, and therefore conclusions about the relative value of $(CV)^2$ at two different depths are applicable as well as the relative value of σ^2 at these depths.

```
C       PROGRAM 1
C       PROGRAM CONVERT(INPUT,OUTPUT,PUNCH)
C       AVGX IS THE AVERAGE DISTANCE DISTANCE THE RECORDING
C       DRUM ADVANCES PER ONE HOUR REAL TIME, I.F. THE DATA
C       SAMPLING RATE,
        DIMENSION U(6000),V(6000),N(80),IBUFF(5000),NK(80)
        IK=0
        READ 97,L
   97 FORMAT(I2)
        READ 98,AVGX
   98 FORMAT(F10.0)
        READ 96,IFILE
   96 FORMAT(I2)
        DO 116 JJ=1,L
        DELT=36.0/AVGX
        PRINT 99,DELT
   99 FORMAT(1H0,2X,25H SAMPLING INTERVAL EQUALS, 1X,E15.7,
       11X,7HSECONDS)
        PRINT 700,JJ
  700 FORMAT(1H0,9HJJ EQUALS, 2X,I2)
        DO 100 I=1,5500
        U(I)=0.0
  100 V(I)=0.0
  101 DO 202 I=1,5000
  202 IBUFF(I)=0
        COUNTX=0.0
        COUNTY=0.0
        NUM=5000
        M=1
        K8=0
        CALL LIOF(5LRBCD1,IBUFF,NUM,NPAR,NEOF)
        IF(NEOF) 602,200
  200 K=-7
        KF=0
  201 K=K+8
        KA=K+8
        KC=0
        DO 102 KB=K,KA
        KC=KC+1
        NK(KC)=IBUFF(KB)
  102 IF (NK(KC).EQ.0) KF=1
        DECODE(80,103,NK) (N(I),I=1,80)
  103 FORMAT(80R1)
        DO 104 I9=1,80
        IF(N(I9).EQ.50B) GO TO 106
        IF(N(I9).EQ.55B) GO TO 107
        IF(N(I9).EQ.34B) GO TO 108
C       SYMBOL / (50) REPRESENTS AN INCREMENT TRAVEL IN THE
C       MINUS X OR Y DIRECTION BY THE DIGITIZER.
C       SYMBOL 0,(55B), REPRESENTS A ZERO INCREMENT TRAVEL
C       IN THE X OR Y DIRECTION BY THE DIGITIZER
C       SYMBOL 1,(34B), REPRESENTS AND INCREMENT TRAVEL IN
C       THE POSITIVE X OR Y DIRECTION BY THE DIGITIZER
C       SYMBOL *,(47B), IS A FLAG INSERTED IN IN THE RECORD
C       BY THE PERSON DIGITIZING BY USE OF THE IRG
        GO TO 104
  106 RX=-0.01
        K8=K8+1
        GO TO 109
  107 RX=0.0
        K8=K8+1
        GO TO 109
  108 RX=0.01
        K8=K8+1
  109 K3=K8/2
        K3=2*K3
        IF(K3.EQ.K8) GO TO 111
        COUNTX=COUNTX+RX
        IF(COUNTX.NE.0.0) GO TO 110
        GO TO 104
  110 U(M)=COUNTX
        GO TO 104
```

```
  111 COUNTY=COUNTY+RX
      IF(COUNTX.NE.0.0) GO TO 112
      GO TO 104
  112 V(M)=COUNTY
      COUNTX=0.0
      M=M+1
      IF(M.GT.6000) GO TO 600
  104 CONTINUE
      IF(KF.EQ.1) GO TO 113
      GO TO 201
  113 MAX=M-7
  105 PRINT 205,M,I9
  205 FORMAT(1H0,2I10)
C     TOTAL TIME OF THE RECORD EQUALS NUMBER OF DATA
C     POINTS TIMES THE SAMPLING INTERVAL, DELT.
      TIME=(M*DELT)/3600.0
      PRINT 115,TIME
  115 FORMAT(1H,10X,26H TOTAL TIME OF RECORD EQUALS,2X,
     1E15.7,2X,7H HOURS.)
      PRINT 215,(V(I),I=1,M)
      PRINT 215,(U(I),I=1,M)
  215 FORMAT(1H ,10X,14F7.2)
      PUNCH 213,(V(I),I=1,M)
  213 FORMAT(14F5.2)
      PUNCH 2100
 2100 FORMAT (20H********************)
  116 CONTINUE
      STOP
  600 PRINT 601
  601 FORMAT(1H0,20X,37H***** U AND V SPACE INADEQUATE ***,)
  602 IK=IK+1
      IF(IK.GT.IFILE)603,200
  603 STOP
      END
```

```
      PROGRAM II
C     RUN 4 DEPTH=14.3 METERS
C     PROGRAM FOR THE SPECTRAL ANALYSIS OF APERIODIC RECORDS
C     DATA MUST BE SAMPLED AT EQUAL INTERVALS OF DT
C     CALCULATES EITHER THE AUTO SPECTRA OR THE CROSSSPECTRA
C     IF NFLAGI=0 ; AUTOSPECTRA. ;IF NFLAGI=1    COSPECTRA
C     IF NFLAGP = 1 . .....CALL PRESS. . ; TOTE
C     IF NFLAGC  = 1 . .....CALL URMS
C     NTS= NUMBER OF TIME SAMPLES
C     MLAG = NUMBER OF TIME LAGS
C     DT = TIME INCREMENT
C     DHZ = FREQUECY SPACING
C     FBHZ = LOWEST FREQUENCY (HZ)
C     FEHZ = HIGHEST FREQUENCY OF INTEREST (HZ)      -
C     TM =DT*MLAG
C     DHZ = 1/(2*A*TM)
C     FEHZ = B/(2*TM)=  B/(2*MLAG*DT)
C     FEHZ = A*B*DHZ
C     A*B = TOTAL NO. FREQUENCY SPACINGS OF ENERGY SPECTRUM
C     A AND B ARE INTEGER CONSTANTS
C     TRANS- INSTRUMENT AND REMARKS
      REAL*8 F1( 6000),F2( 6000),ITITEL(12),ITITIL(12)
      DIMENSION F1( 6000),F2( 6000),SPHI(600),APHI(600),PHN(600)
      DIMENSION PHI(6000),TAU(600),CYCL(700),SPEC(700),SSP(700)
      DIMENSION CSPEC(700),QSPEC(700),SS2(700),PHASE(700),COHER(700)
      DIMENSION RESPF(700),PER(700),SPE2(700),TRANS(10)
      DIMENSION DATE(2),HOUR(2),LABLI(4HQUAD/,MONT,LABIL/4H PHI/,LABLE/4HCROS
      REAL*4 LABEL/4H CO /,LABLE(4H PHI/,LABLE/4HCROS
  1/  CONTINUE
 999  READ(5,200,END=888) (ITITLE(I),I=1,12)
      READ(5,200,END=888) (ITITEL(I),I=1,12)
 200  FORMAT(6A8) DATE,HOUR,TRANS
      READ(5,802) DATE,HOUR,TRANS
 802  FORMAT(2A4,2A4,10A4)
      READ(5,96) NFLAGI,NFLAGP,NFLAGC
      READ(5,99) NTS,MLAG,DT,DHZ,FBHZ,FEHZ
      READ(5,801) CALX1,CALX2,H,X2,AZZ,S
      WRITE(6,811)
 811  FORMAT(1H1)
      WRITE(6,803)  DATE,HOUR,TRANS
      WRITE(6,98) NTS,MLAG,DT,DHZ,FBHZ,FEHZ,CALX1,CALX2,H,X2
 96   FORMAT(3I6)
 98   FORMAT(7H NTS = ,I6//,8H MLAG = ,I6//,6H DT = ,F9.5//,6H DHZ= ,F10
     1.8//, FBHZ = ,F10.8//, FEHZ = ,F12.8//, CALX1= ,F10.8//,
     2. CALX2 = ,F10.8//, H = ,F10.3//, X2 = ,F10.3//)
 99   FORMAT (2I6,5F10.8)
```

```
801 FORMAT(6F10.5)
803 FORMAT(40H LONG WAVE STUDY OF MONTEREY BAY          ,5X,7H DATE   ,2A
   14,10H     HOUR   ,2A4/,5X,10A4///)
C BAND WIDTH FREQUENCIES OF TOTAL ENERGY FLUX- CMIN,CMAX
   CMIN = 0.0
   CMAX = 0.2
C
C COMPUTING POWER SPECTRUM
   PI=3.1415926 5
   FB = FBHZ*2.0*PI
   FE = FEHZ*2.0*PI
   DF = DH7 *2.0*PI
   FMIN = .0*PI*CMIN
   FMAX = 1.0*PI*CMAX
900 FORMAT(14F5.2)
   READ(5,900)(F1(I),I=1,NTS)
   XMAX = F1(1)
   DO 23 I=2,NTS
   IF(XMAX.GE.F1(I)) GO TO 23
   XMAX = F1(I)
23 CONTINUE
   DO 24 I=1,NTS
   F1(I)=((F1(I)-XMAX)*(-.212))
24 CONTINUE
   WRITE(6,901)(F1(I),I=1,NTS)
901 FORMAT(14F7.2)
   CALL TREND(F1,NTS,DT,CALX1)
21 DO 10 M=1,MLAG
   SUM=0.0
   NMAX=NTS-M+1
   DO 8 I=1,NMAX
   NN=M+I-1
8  SUM=SUM+F1(I)*F1(NN)
   XNMAX=NMAX
   XX=M-1
   TAU(M)=XX*DT
   PHI(M)=SUM/XNMAX
   WRITE(6,300)(PHI(1))
300 FORMAT(5X,'PHI(1)=',F20.5)
   PHN(M) = PHI(M)/PHI(1)
10 CONTINUE
   CALL PARZ(MLAG,PHI)
798 FORMAT(' PHI(0) = ',F10.4//)
   NFREQ=(FE-FB)/DF+0.1
   DO 14 N=1,NFREQ
   XN=N
   FREQ(N)=(XN-1.0)*DF+FB
14 CYCL(N) = FREQ(N)/(2.0*PI)
```

78

```
      PER(1) = 0.0
      DO 15 N = 2,NFREQ
   15 PER(N) = 1.0/CYCL(N)
      MLAGM1=MLAG-1
      XMLAG=MLAG
      DO 50 N=1,NFREQ
      SUM=0.5*(PHI(1)+PHI(MLAG)*COS(FREQ(N)*TAU(MLAG)))
      C1=COS(FREQ(N)*DT)
      S1=SIN(FREQ(N)*DT)
      CC=1.0
      SC=0.0
      DO 49 M=2,MLAGM1
      CT=CC*C1-SC*S1
      ST=SC*C1+CC*S1
      CC=CT
   49 SC=ST
   50 SUM=SUM+PHI(M)*CC
      SPEC(N)=(SUM*2.0/XMLAG)
      IF(NFLAGP) 741,741,742
  742 CONTINUE
      CALL PRESS(FREQ,SPEC,NFREQ,H,X2,DF,FB,FMAX)
  741 CONTINUE
      MD=3.14159265/(DF*DT*XMLAG)+0.1
      CALL SMO(MD,SPEC,SSP,NFREQ)
C SUBROUTINE TO CALCULATE VARIANCE
      DC = DF/(2.0*PI)
      SUM = 0.0
      DO 650 N=1,NFREQ
  650 SUM = SUM + SPEC(N)
      WRITE(6,651) SUM
  651 FORMAT(25H        VARIANCE OF SPECTRUM//,3X,16H        VARIANCE = ,F10.
     17,10H        M2         //)
      IF(NFLAG1) 743,743,744
  744 CONTINUE
  743 CONTINUE
      DO 700 III=1,NFREQ
  700 SPEC(III)=10*ALOG10(SPEC(III))
      WRITE(6,106)(TAU(M),PHN(M),M=1,MLAG)
  105 FORMAT (10X,24H ENERGY SPECTRAL DENSITY//,5X,10H FREQUENCY,5X,13H
     1 RAW SPECTRUM,3X,18H SMOOTHED SPECTRUM//)
      CALL DRAW(250,CYCL,SPEC,0,0,LABEL,ITITLE,0.0,0.0,0.0,0.8,8,1,
     1LAST)
      CALL DRAW(480,TAU,  PHN,0,0,LABEL,ITITEL,0.0,0.2,2,0.8,8,1,
     1LAST)
  106 FORMAT (5X,F10.5,6X,F10.5)
      WRITE(6,105)
      WRITE(6,106)(CYCL(M),SPEC(M)           ,M=1,NFREQ)
  108 FORMAT(2F10.8)
```

79

```fortran
109 FORMAT (I6)
888 RETURN
    END

C   SUBROUTINE PRESS(FREQ,SPEC,NFREQ,H,X2,DF,FB,FMAX)
C   SUBROUTINE TO CONVERT PRESSURE SPECTRUM TO ENERGY SPECTRUM
    DIMENSION FREQ(NFREQ),SPEC(NFREQ)
    NMAX = (FMAX-FB)/DF+1.0
    DO 11 I=1,NMAX
C   CALCULATE LINEAR WAVE LENGTH BY NEWTONS METHOD
7   XKHO = FREQ(I)*H/9.80
    IF(FREQ(I)-0.0001) 8,8,7
    IF(XKHO-6.3) 5,1,1
1   XKH = XKHO
    GO TO 9
5   XKH = SQRT(XKHO)
3   SH = SINH(XKH)
    CH = COSH(XKH)
    EPS = XKHO-XKH*SH/CH
    SLOPE = -XKH/CH**2-SH/CH
    DXKH = -EPS/SLOPE
    IF(ABS(DXKH/XKH)-0.0001) 9,9,4
4   XKH = XKH+DXKH
    GO TO 3
8   RESPF = 1.00
    GO TO 12
9   XK = XKH/H
    RESPF = COSH(XK*H)/(COSH(XK*(H-X2)))
    IF(RESPF-10.0) 11,11,12
11  SPEC(I) = RESPF*RESPF*SPEC(I)
12  RETURN
    END

    SUBROUTINE TREND(FX,NTS,DT,CALXX)
    DIMENSION FX(NTS)
C   CALIBRATIONG RECORD
    DO 104 I=1,NTS
104 FX(I) = FX(I)*CALXX
C   COMPUTING THE LINEAR TREND
    FNTS = NTS
    SUMF = 0.0
    DO 101 I=1,NTS
101 SUMF = SUMF + FX(I)
    SUMF1 = 0.0
    DO 102 I=1,NTS
    XI = I
```

```
102 SUMF1 = SUMF1 + XI*FX(I)
    XNM1 = NTS-1
    XNP1 = NTS+1
    XM = (1.0/DT)*(12.0*SUMF1/(FNTS*XNM1*XNP1)-6.0*SUMF/(XNM1*FNTS))
    B = SUMF/FNTS-XM*XNP1*DT/2.0
    FMEAN = SUMF/FNTS
    WRITE(6,9) FMEAN,XM,B
  9 FORMAT (3X,8H MEAN = ,F10.5,3X,9H SLOPE = ,F10.5,3X,13H INTERCEPT
   1= ,F10.5/)
    DO 103 I=1,NTS
    XI = I
103 FX(I) = FX(I) - (B+XM*XI*DT)
    RETURN
    END

    SUBROUTINE SMO(MD,X1,X2,NFREQ)
    DIMENSION X1(MD),X2(MD)
    DO 1 N=1,MD
    NA=N+MD
    NN=NFREQ-N+1
    NB=NN-MD
    X2(N) = 0.25*(X1(1)+X1(NA))+0.5*X1(N)
  1 X2(NN)=0.5*(X1(NN)+X1(NB))
  3 MB=MD+1
    ME=NN-1
  5 DO 2 N=MB,ME
    NA=N+MD
    NB=N-MD
  2 X2(N)=0.25*(X1(NA)+X1(NB))+0.5*X1(N)
    RETURN
    END

    SUBROUTINE PARZ(MLAG,PHI)
    PARZ SUBROUTINE PARZEN FILTERS AUTO-CORRELLATION FUNCTION
    DIMENSION PHI(MLAG)
    XMLAG = MLAG
    MLAGH = XMLAG/2.0-0.1
    MLAGH1 = MLAGH + 1
    DO 31 M=1,MLAGH
    MM = M-1
    R = MM
    RM = R/XMLAG
    UM = 1.0-6.0*RM*RM*(1.0-RM)
    PHI(M) = PHI(M )*UM
 31 CONTINUE
    DO 32 M = MLAGH1,MLAG
```

```
      MM = M-1
      R = MM
      RM1 = R/XMLAG
      RM1 = (1.0-RM)
      UM = 2.0*RM1*RM1*RM1
      PHI(M) = PHI(M)*UM
   32 CONTINUE
      RETURN
      END
```

```
C          PROGRAM IV
C          PROGRAM TO CALCULATE THE VARIANCE OF THE FRACTIONAL
C          MODULATION OF EACH RUN.
           DIMENSION X(5600)
           READ (5,1100)(X(I),I=1,5600)
  1100     FORMAT(14F5.2)
           XMAX=X(1)
           DO 23 I=2,5600
           IF (XMAX.GE.X(I)) GO TO 23
           XMAX=X(I)
    23     CONTINUE
           DO 24 I=1,5600
           X(I)=(X(I)-XMAX)*(-.212)
    24     CONTINUE
           X3=0.0
           DO 30 I=1,5600
           X3=X3+(X(I)**2)
    30     CONTINUE
           X3=X3/5600
           WRITE(6,99)(X3)
    99     FORMAT(5X,'MEAN SQUARE=',F5.4)
           X4=0.0
           DO 31 I=1,5600
           X4=X4+X(I)
    31     CONTINUE
           X4=X4/5600
           WRITE(6,100)(X4)
   100     FORMAT(5X,'MEAN=',F5.4)
           X5=X4**2
           X6=X3-X5
           WRITE(6,101)(X6)
   101     FORMAT(5X,'SIGMA SQUARE=',F5.4)
           STOP
           END
```

BIBLIOGRAPHY

1. A.D. Little Report 1360863, <u>Project Trident Report: Acoustic Scattering in the Ocean</u>, by R.F. Meyer and B.W. Rimberg, August 1963.

2. Bobber, R.J., <u>Underwater Electroacoustic Measurements</u>, U.S. Government Printing Office, 1970.

3. Campanella, S.J., and Favret, A.G., "Time Auto-correlation of Sonic Pulses Propagated in a Random Medium", <u>The Journal of the Acoustical Society of America</u>, V. 46 no.5 (part 2) p. 1234-1245, November 1969.

4. Horton, C.W., <u>Signal Processing of Underwater Acoustic Waves</u>, U.S. Government Printing Office, 1969.

5. Kaufman, C., "Scattering of Sound by Underwater Turbulence", <u>Journal of the Acoustical Society of America</u>, v. 49 no.3 (part 2), 1971.

6. Kennedy, R.M., "Phase and Amplitude Fluctuations in Propagating through a Layered Ocean", <u>The Journal of Acoustical Society of America</u>, V. 46, no. 3 (part 2), pp. 737-745, March, 1969.

7. Kinsler, L.E., and Frey, A.R., <u>Fundamentals of Acoustics</u>, Wiley, 1962.

8. LaCasce, E.O., Jr., Stone, R.G., and Mintzer, D., "Frequency Dependence of Acoustic Fluctuations in a Randomly Inhomogeneous Medium", <u>Journal of Applied Physics</u>, v. 33 no. 9, pp. 2710-2714, September, 1962.

9. Medwin, H., <u>Notes on Underwater Acoustics Section 5.2 Bubble Resonance</u>, paper presented for course PH 4454, Naval Postgraduate School, January, 1971.

10. Stone, R.G., and Mintzer, D., "Transition Regime for Acoustic Fluctuations in a Randomly Inhomogeneous Medium", <u>Journal of the Acoustical Society of America</u>, v. 38 no. 5, p 843-846, November, 1965.

11. Thomas, John B., <u>Statistical Communication Theory</u>, Wiley, 1969.

12. Urick, R.J., <u>Principles of Underwater Sound for Engineers</u>, McGraw-Hill, 1967.

13. Whitmarsh, D.C., Skudrzyk, E., and Urick, R.J., "Forward
    Scattering of Sound in the Sea and Its Correlation
    with the Temperature Microstructure", The Journal of
    the Acoustical Society of America, v. 29 no. 10,
    p. 1124-1143, October, 1957.